Analysis of neuronal differentiation mechanism in iPS・EC cells

Dissertation

Analysis of neural differentiation mechanism in iPS・EC cells

(iPS·EC 細胞における神経細胞分化機構の解析)

Division of Life Sciences

Graduate School of
Natural Science & Technology
Kanazawa University

Student ID No. 1023032521

Name: JULIET OBANDA MAKANGA

Chief advisor: YUKIO YONEDA

Date of Submission: 9th January 2015

CONTENTS

ABSTACT

Embryonic stem (ES) cells are undifferentiated cells derived from embryos. ES cells possess the ability to proliferate and self-renew indefinitely and are able to differentiate to cells of three germ layer. However, they are technically difficult to handle and are ethically controversial. Yamanaka and his group succeeded in reprogramming somatic cells into pluripotent state by forced expression of transcription factors establishing induced pluripotent stem (iPS) cells. iPS cells are similar to ES cells but are advantageous as they can be a source of patient/model specific cells. Embryonal carcinoma (EC) cells are also similar to ES cells but are malignant. Given their pluripotent nature, iPS and EC cells serve as valuable alternatives to ES cells in the study of pluripotency and differentiation mechanisms such as neurogenesis.

Neurogenesis is the process through which new nerve cells are generated from neural progenitor cells and has been reported to persist even in the adult nervous system. As is the case with other development processes, neurogenesis is a complex process intricately modulated by mechanisms yet to be fully understood. Alterations in neurogenesis interferes with brain development, function resulting to cognitive deficits and neurological conditions.

On the other hand, chromatin modulators such as histone deacetylase (Hdac) inhibitors have been used to improve reprogramming efficiency during iPS cell generation. Changes in histone acetylation status affect gene expression in turn controlling proliferation, differentiation and development. Hdacs consist of a number of isoforms that regulate cellular mechanisms differently. Hdac8 is an isoform expressed in the brain and in neuroblastoma and is associated with poor prognosis.

This research aimed to 1) generate rat iPS cells using a non-viral plasmid vector and establish a protocol to differentiate them to neural lineage and 2) investigate the role of selectively inhibiting

Hdac8 on neurogenesis using retinoic acid treated P19 EC cells as a model.

We successfully generated rat iPS cells (riPSC) and applied a multi-step protocol to differentiate riPSC to a neuronal lineage comprising of glutamatergic and dopaminergic neurons. Glutamatergic neurons were responsive to agonist stimulation. We also found a novel glycophenotypic difference in expression of epitopes that bind R-10G antibody, which reacts with human ES/iPS cells but not EC cells. riPSC clone highly reactive to R-10G formed teratomas consisting of derivatives of all three germ cell layers. On the other hand, low reactive clones resulted in tumor masses made up of undifferentiated cells. Conventionally used tumor rejection antigen (TRA)-1-81 epitope expression was comparable.

In the second part of the study, we found HDAC8 inhibition suppressed proliferation, reducing size of P19 cell aggregates and 2-(2-methoxy-4-nitrophenyl)-3-(4-nitrophenyl)-5-(2,4-disulfophenyl)-2H-tetrazolium (WST-8) reducing activity without inducing cell death. Anti-proliferative effect was characterized by upregulation of the cell cycle inhibitor p21 and mRNA expression. HDAC8 inhibition also resulted in downregulation of Sox2 protein level as well as Musashi-1 and repressor type bHLH factor, Hes5, mRNA expressions.

The establishment of rat iPS cells and differentiation into neuronal lineage cells provides a model to help study neurogenesis processes as well as pharmacological and toxicological studies on neurons. Glygophenotypic difference with regard to R-10G found is potentially useful for rat iPS cell evaluation and to study the role of glycans in pluripotency and carcinogenesis in these cells. The findings of the second part of this thesis, uncover as well as suggest a role for HDAC8 inhibition in proliferation and probably neurogenesis in pluripotent P19 cells.

PART 1: Generation of rat iPSC and differentiation to neuronal lineage cells.

INTRODUCTION

Yamanaka and his group opened a new era in stem cell science with the generation of induced pluripotent stem cells (iPSC) by the overexpression of transcription factors, *octomer 3/4 (Oct3/4)*, *SRY box-containg gene 2 (Sox2)*, *c-Myc (myelocytomatosis cellular oncogene)* and *Kruppel-like factor 4 (Klf4)* in mouse embryonic fibroblasts (MEF) (Takahashi and Yamanaka, 2006). Since then iPSC have been generated from human (Takahashi K.*et al.,*2007), monkey (Liu H. *et al,* 2008), pig (Esteban *et al*. 2009), sheep (Bai *et al.* 2008) and rat (Li W. *et al,* 2009) among other mammalian species. iPSC are similar to embryonic stem cells (ESC) in regard to ability to self-renew and differentiate into a variety of cells. iPSC are derived from somatic cells hence they offer an alternative to ESC that are technically difficult to establish and make use of embryos raising ethical concerns. However, iPSC equivalency to ESC is still much debated.

The rat has been useful as an animal model in many research fields (Jacob HJ. *et al.,* 2010). Data from studies using rat models has formed a foundation for investigations into disease mechanism and therapeutic strategies. Despite authentic mouse ESC having been derived more than three decades ago (Evans and Kaufman, 1981), rat ESC were only recently established (Buehr M. *et al.,*2008; Li P. *et al*., 2008) making it possible to generate rats with genetic modifications (Tong C. *et al.* 2010). Several rat iPSC lines have been established (Liao J. *et al.,* 2009; Li W. *et al,* 2009; Chang MY. *et al.,* 2010; Liskovykh M. *et al.,* 2011) and transgenic rats generated from rat iPSC (Jiang MG. *et al.,*2013). Hence, rat iPSC development is indeed a step forward. However, rat iPSC lines reported were generated via viral transduction of reprogramming factors which has disadvantages such as proviral integrations in resulting iPSC.

Variation observed among iPSC of not only species of origin, but also reprogramming methods,

culture conditions and laboratory-specific variations remains a concern (Okita and Yamanaka 2012). Issues regarding pluripotency, differentiation and tumorigenic propensity remain a challenge especially in employment of these cells for therapeutic purposes.

Cell surface glycans are often referred to as cell signature and different cell types express different glycan patterns which vary during differentiation and various biological processes such as cancer (Sjoberg and Varki, 1993; Dodla MC. *et al.,* 2011; Li M. *et al.,* 2010). In this light, cell surface glycans are considered ideal targets for identifying and characterizing cellular phenotype. Cell surface glycans such as stage-specific embryonic antigens (SSEA)-3/4 and tumor rejection antigen (TRA)-1-60/81 are routinely used to evaluate pluripotency. However, these glycans are not unique to ESC and iPSC but are also expressed in embryonal carcinoma (EC) cells (Kannagi R. *et al.,* 1983; Andrews PW. *et al.,* 1984). Kawabe K. *et al*. generated a monoclonal antibody, R10-G, by using a human iPS cell line (Kawabe K. *et al*. 2013). The epitope binding R-10G was identified as a type of keratan sulfate similar to TRA-1-81 epitope but possessed unique properties. Moreover, this antibody only recognized human ES and iPS cells but not EC cells. Characterization of cell surface glycans in iPSC potentially offers a tool to elucidate changes that occur during reprogramming as well as the role of glycans in acquisition and maintenance of pluripotency and stemness.

Aim: To generate rat iPSC (riPSC) using a non-viral plasmid vector introduced via electroporation and differentiate riPSC to neural lineage cells.

RESULTS

Generation of riPSC and characterization.

First, primary fibroblasts were prepared from skin biopsies of adult male Wistar rats and passaged twice at most prior to the reprogramming experiments. We introduced 8μg of pCAG2LMKOSimO vector into 1.1×10^6 cells as described in the methods section. We then plated the fibroblasts on inactivated MEFs and cultured them in LIF and 400μg G418 containing media. Colonies were visible from about day 7 post transfection. We picked a total of 11 colonies over a time span ranging from 14 to 20 days post transfection. The colonies were expanded during when we closely observed aspects such as colony morphology, growth rate, and presence of foci of increased growth as signs for similarity to ES cells. Figure 1 shows phase contrast images of source cells, adult rat fibroblasts and representative image of colonies.

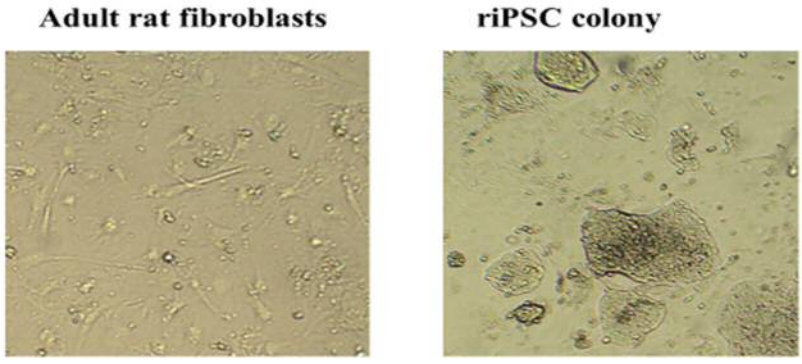

Figure 1. Source cells, adult rat fibroblasts and representative image of rat iPS cells (riPSC) cultured on mouse embryonic fibroblasts (MEFs).

ES cell colonies are known to have characteristic round bodies with sharp edges. Initially, our riPSC clone colonies seemed to be unsatisfactory in this light. This lead us to attempt the LIF+2i approach which Silvia et al. reported to induce transition of intermediate reprogramming states to ground state pluripotency in mouse iPS cells. 2i, CHIR99021 and PD0325901, are two small molecule inhibitors of the MAPK (mitogen activated protein kinase)/Erk (extracellular signal regulated kinases 1 and 2) pathway and GSK3 respectively. Indeed, this same approach successfully allowed the derivation of ES cell lines from rats which had been elusive for a long period of time (Buehr M *et al,* 2008; Li P *et al*, 2008). Addition of 2i to the culture system dramatically improved morphology of riPSC colonies. Hence, further culture was carried out in media containing LIF+2i.

We next embarked on examining the ES cell like features and characterizing the riPSC clones. A useful tool for identifying pluripotency in initial phases of reprogramming is alkaline phosphatase (AP) staining (Brambrink, 2008). AP is a hydrolase enzyme that under alkaline conditions dephosphorylates nucleotides and proteins and elevated levels is associated with pluripotent phenotypes (Thomson and Marshall, 1998). riPSC clones were cultured on MEFs and stained for AP after 3 days. Figure 2 shows riPSC colonies stained for AP (reddish purple appearance) while rat fibroblasts, the source cells were unreactive (clear appearance) indicating riPSC were of a pluripotent nature. In the cause of propagating the colonies, we selected a three clones to carry downstream experiments namely riPSC#3, #6 and #11 as other clones showed poor propensity and could not be maintained in culture.

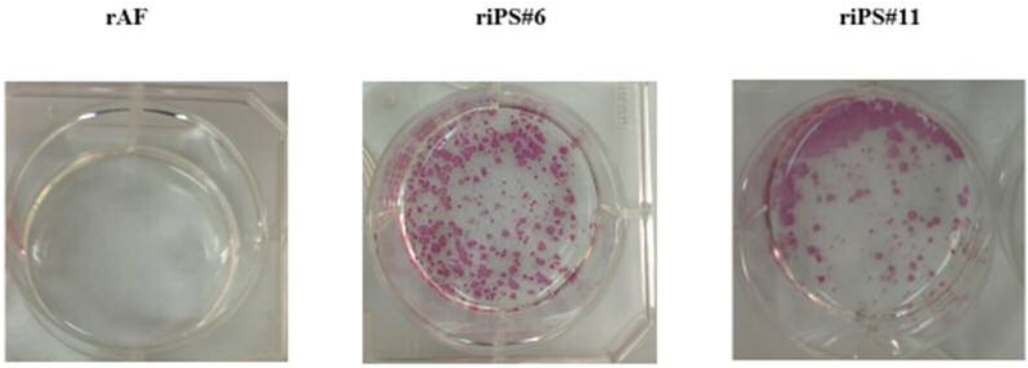

Figure 2. Alkaline Phosphatase (AP) Staining. AP staining of adult rat fibroblasts, riPSC#6 and riPSC#11.

Next, we carried out immunocytochemical staining for ES cell marker, Nanog, surface marker and stage-specific embryonic antigen, SSEA1. riPSC were passaged and cultured for 5 days before fixation with 4% PFA and then immunoreacted with respective antibodies. Consistent with studies carried out on rat ES cells, the riPSC clones expressed Nanog (nuclear localized) and SSEA-1 (cell surface localized) (Figure3). Control experiments showed rAF were unreactive. Furthermore, Nanog and SSEA-1 expression were confirmed in riPSC clones after multiple passages (Figure 4.)

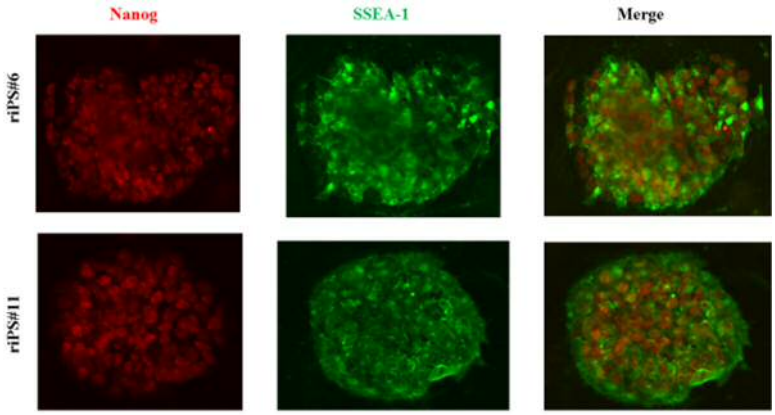

Figure 3. Characterization of riPSC. Nanog and SSEA-1 expression in riPSC#6 and riPCS#11 were determined by immunocytochemistry.

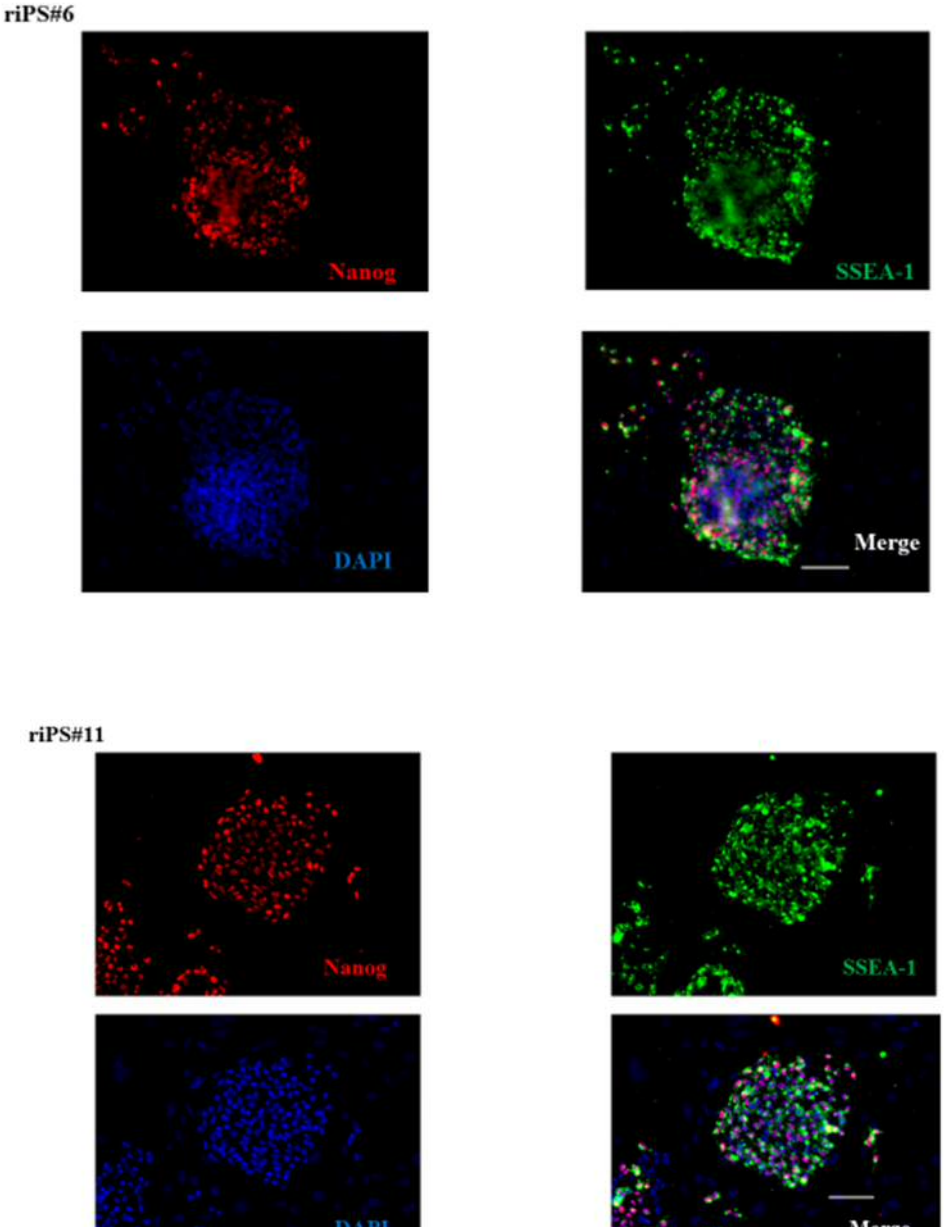

Figure 4. Characterization of riPSC. Nanog and SSEA-1 expression in riPSC#6 and riPCS#11 respectively, were determined by immunocytochemistry after multiple passages.

Furthermore, we assessed expression of endogenous transcripts for pivotal pluripotency genes by RT-PCR. Figure 5 shows riPSC clones expressed these genes whose expression was undetected in rat fibroblast samples. Taken together, these data confirmed reprogramming had indeed taken place.

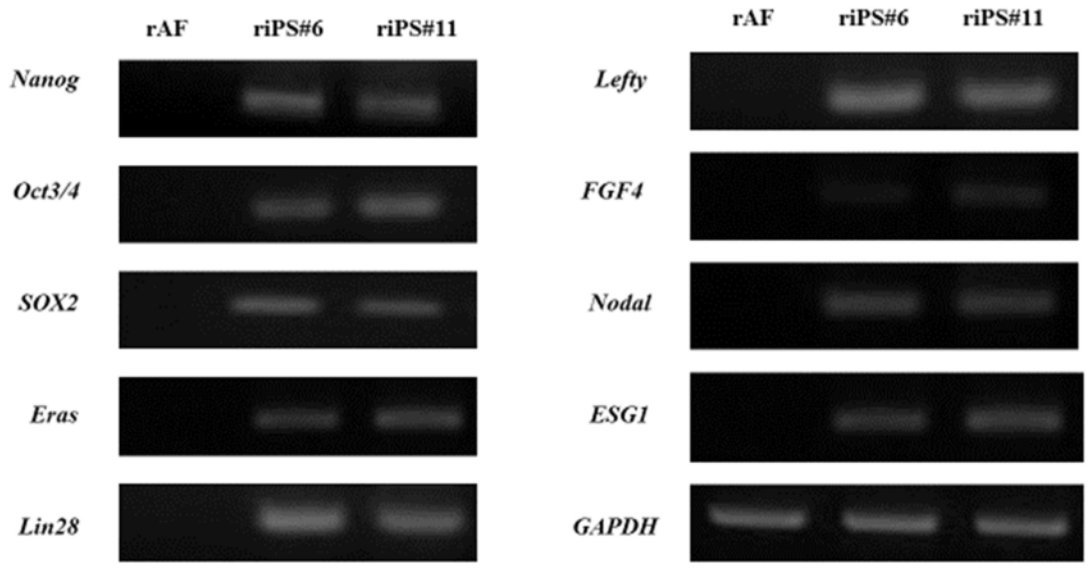

Figure 5. Characterization of riPSC. RT-PCR analysis of ES marker genes. riPSC express endogenous ES marker genes. Source cells (rAF) were used as negative control. *GAPDH* was used as loading control.

The conversion of somatic cells into iPS cells during the reprogramming process is accompanied by epigenetic changes including demethylation of promoter and enhancer regions of pluripotency genes such as Oct3/4. We therefore examined the methylation status of the rat Oct3/4 promoter region (-1495 to 1290 bp) by bisulfite sequencing. Bisulfite sequencing involves the denaturing of genomic DNA followed by treatment of DNA with sodium bisulfite that results into conversion of unmethylated cytosine residues to uracil. Methylated cytosine residues remain unchanged. PCR amplication using primers specific to the region of interest converts uracil

residues to thymine. PCR products are sequenced determining DNA methylation status.

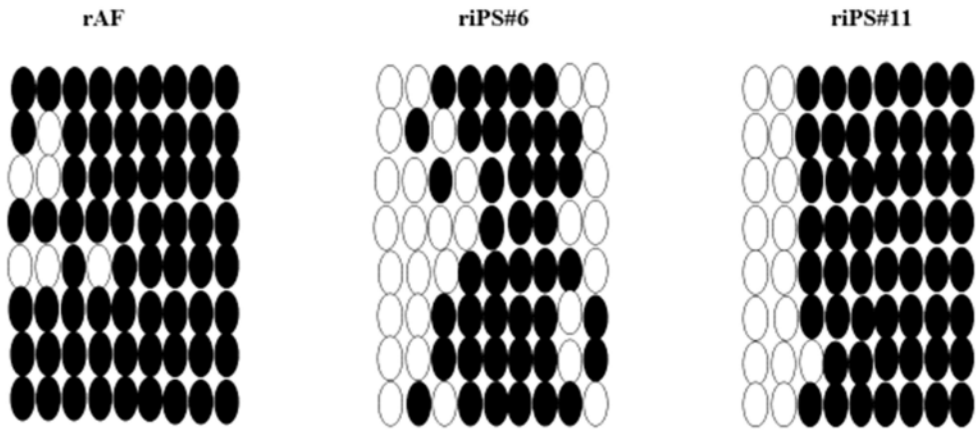

Figure 6. Characterization of riPSC. Bisulfite sequencing of promoter region of rat *Oct3/4.* Open circles represent unmethylated CpGs. Filled circles indicate methylated CpGs.

Our findings revealed a difference in the riPSC clones we had established. riPS#6 was relatively hypomethylated while riPS#11 showed a higher methylation status. This was unexpected given endogenous Oct3/4 transcripts had been detected in the cells. We decided to confirm Oct3/4 protein expression though immunostaining. Cells were passaged and routinely cultured on MEFs for 5 days followed by fixation in 4%PFA and reaction with Oct3/4 antibody. As shown in figure 7, there was no significant difference in Oct3/4 protein expression levels in the clones.

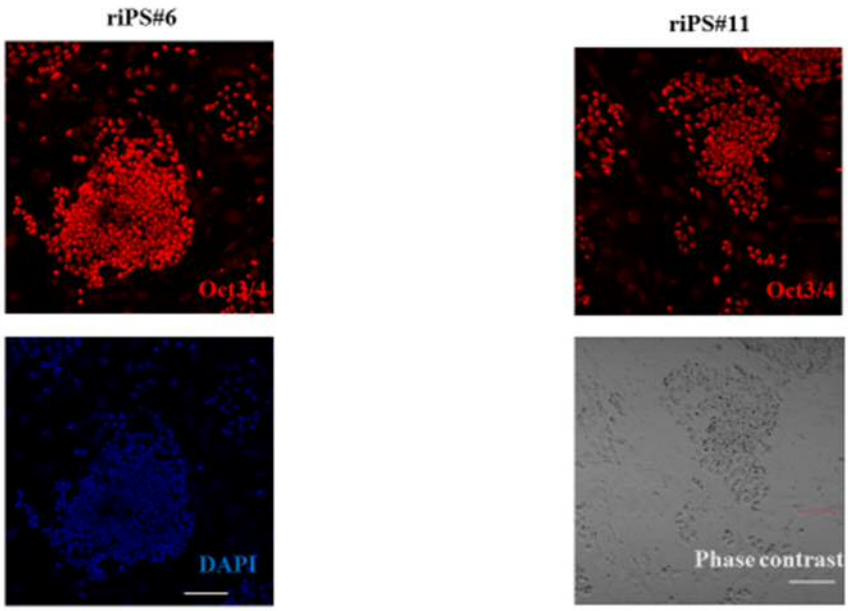

Figure 7. Characterization of riPSC. Immunocytochemical analysis of Oct3/4 expression in riPSC#6 and riPSC#11. riPSC clones were homogenously labeled with antibodies against Oct3/4 (red). Nucleus was stained with DAPI (blue).

We also examined karyotypic status of riPSC clones after repeated passages. Metaphase spreads were prepared and 100 spreads were counted for each riPSC clone. riPS#6 had a majority (60%) of normal karyotype (2n=42) spread. Contrastingly, riPS#11 and riPS#3 had mostly aneuploidy spreads with an increase in the number of chromosomes of up to 64.

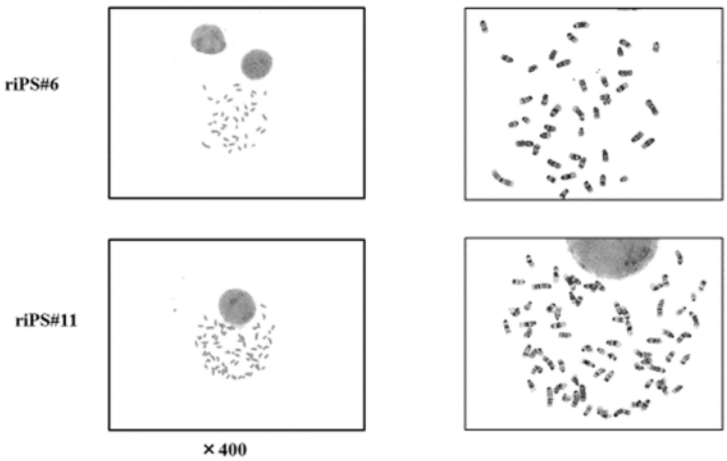

Figure 8. Characterization of riPSC. Representative metaphase spreads of riPSC#6 and riPSC#11. riPSC showed majority normal (2N=42) chromosome content. riPSC#11 spreads were mostly abnormal with up to 2N=64 chromosome

Primary somatic cells in their native nature have a limited capacity to be cultured and can only be passaged for a limited duration before they become senescent; a concept first propose by Leonard Hayflick about five decades ago (Shaw JW, Wright WE 2000). iPS cells gain the ability to be expanded and maintained in culture indefinitely making them similar to ES cells in this light. We were able to maintain riPSC in culture for over 15 passages without notable change in morphological appearance.

R-10G reactivity

To characterize the riPSC clones further, we tested the binding of R-10G antibody to the cells. riPSC were routinely cultured on MEFs for 3-5 days and fixed with 4% PFA for immunostaining experiments. Unexpectedly, R-10G binding appeared to be differential in the riPSC. Initially, we used the conventional immunostaining protocol that involved fixation, permeablization, blocking and antibody reaction. As in Figure 9, we were unable to determine clear localization and the immunofluorescence results were unsatisfactory. Nevertheless, riPSC#11 was only lowly reactive to the antibody.

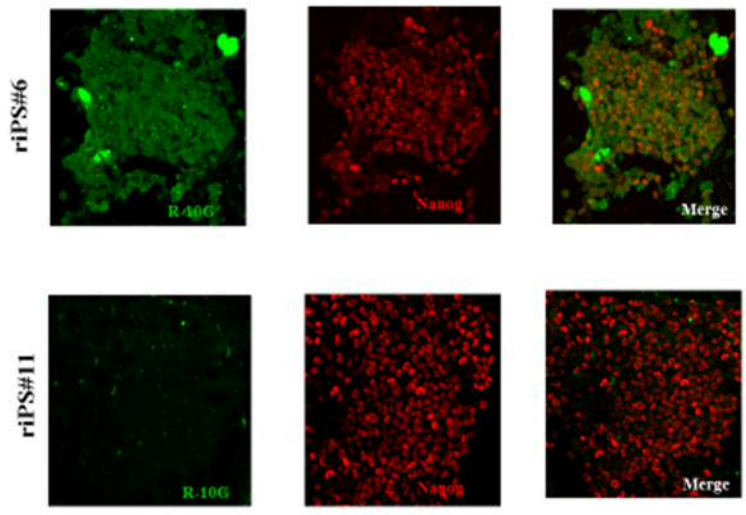

Figure 9. R-10G reactivity. riPSC were fixed, permeabilized and immunoreacted with R-10G (green) and Nanog (red) antibodies. Upper panel shows riPSC#6, lower panel shows riPSC#11.

Since the epitope recognized by R-10G is localized on the cell surface, we decided not to treat the cells with a surfactant, omitting the permeabilization step hence ensuring the cell surface remained intact. With this we successfully obtained clearer images that confirmed riPS#6 showed higher reactivity to R-10G antibody in comparison to other clones (Figure 10).

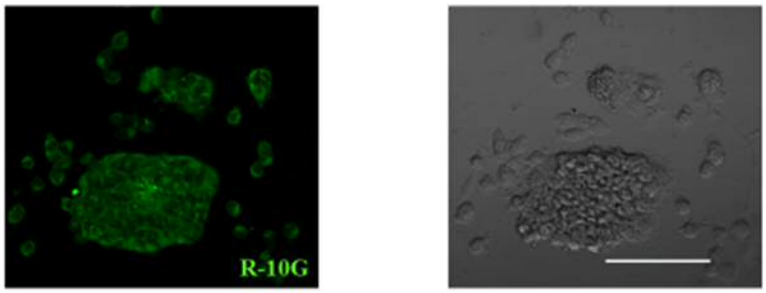

Figure 10. R-10G reactivity. riPSC#6 were fixed in 4% PFA and reacted with R-10G without permeabilization. Left panel: R-10G (green). Right panel: phase contrast image.

Kawabe *et al.* identified the antigen carrying the R-10G epitope as the transmembrane protein podocalyxin (Kawabe *et al* 2013). Podocalyxin consists of a cytoplasmic domain and an extracellular domain which is heavily glycosylated (Sassett *et al.* 2000). Podocalyxin also acts as a carrier protein to the TRA-1-60 and TRA-1-81 epitopes, both of which are conventionally used ES/iPS cell marker antibodies (Schopperle and DeWolf 2007).

Our observations in difference in riPSC clone reactivity to R-10G might have been as a result of (1) differences in R-10G binding epitope expression or (2) differences in carrier protein expression levels. To test these possibilities, we performed immunofluoresence staining using R-10G and TRA-1-81. Cells were cultured routinely on 6cm tissue culture dishes for 4 days and

reacted with respective primary and secondary antibodies. Nuclei were stained with DAPI. Images were acquired using a fluorescent microscope.

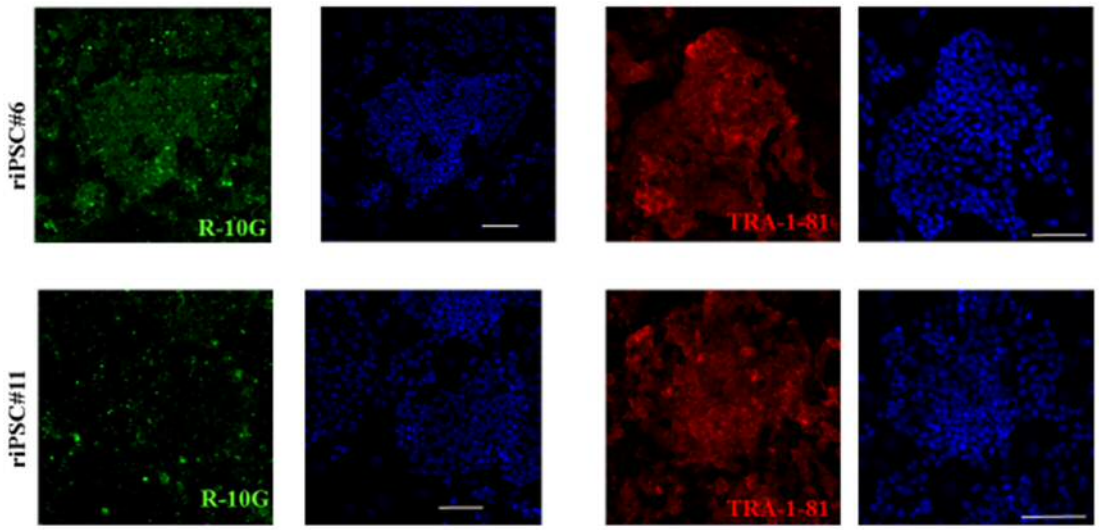

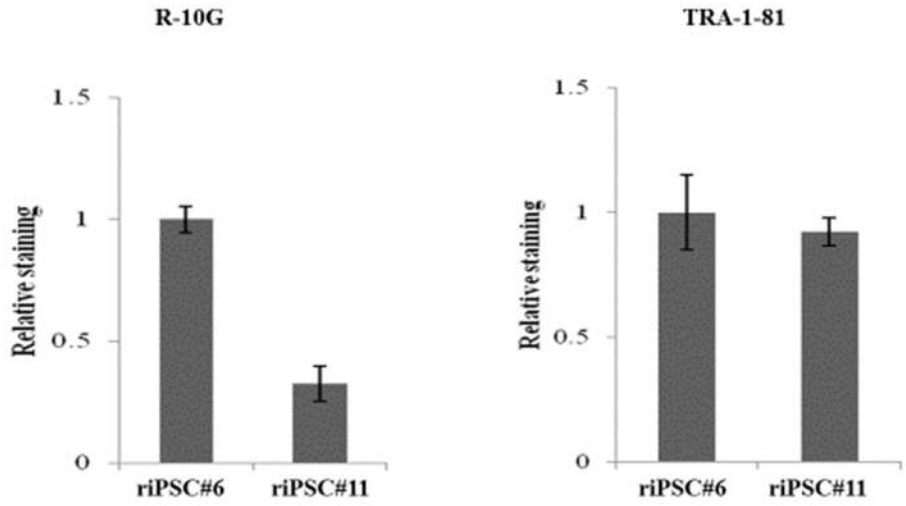

Figure 11. R-10G and TRA-1-81 binding. Upper panel: riPSC#6, Lower panel: riPSC#11 R-10G (green) TRA-1-81 (red) DAPI (blue). Quantification of fluorescence intensity. Results were normalized against DAPI. Results are means ±S.D. of 81 random fields from three independent experiments.

Fluorescence intensity was quantitated using the KEYENCE Hybrid Cell Count BZ-H2C software. Fluorescence intensity for green (R-10G) and red (TRA-1-81) were normalized against blue (DAPI). Results are shown in Figure 11 above. TRA-1-81 bound with riPSC#6 and riPSC#11 in a similar fashion and fluorescence intensity was comparable. Consistent with previous observations, R-10G staining intensity was approximately three times lower in riPSC#11 in comparison with riPSC#6.

***In vitro* differentiation**

R-10G did not bind, 2102Ep and NCR-G3, two human EC cell lines studied (Kawabe *et al* 2013). EC cells which are considered malignant counterparts of ES cells have a limited capacity for differentiation (P.W.Andrews *et al.* 2005). Since we had observed unexpected difference in R-10G binding activity to riPSC clones we generated, investigating their differentiation ability became of great interest. We hypothesized the riPSC clones could vary in their capacity to differentiate. Our next aim was to investigate the differentiation ability of riPSC both *in vitro* and *in vivo*.

For *in vitro* differentiation, cells were mildly dissociated and culture on low attachment dishes in riPS media without LIF and 2i. Cells were contained for 7 days during when they formed spherical aggregates with smooth boundaries. On day 7, we collected the aggregates and treated them with Accutase for mild dissociation. Cells were replated on gelatin coated dishes for spontaneous differentiation. Aggregates successfully attached to culture dishes and we observed morphological change in cell appearance at the outgrowths

To evaluate differentiation, we fixed and stained differentiated riPSC against markers for three

germ layers; α-Fetoprotein (AFP) (endoderm), Smooth muscle actin (SMA) (mesoderm) and βⅢ Tubulin (ectoderm). riPSC clones uniformly gave raise to cells of all three germ layers. Additionally, we isolated RNA samples and performed RT-PCR to detect expression of germ layer specific transcripts; GATA4, SOX17 (endoderm), Fetal liver kinase (flk) (mesoderm) and Neural cell adhesion molecule (Ncam) (endoderm). (data not shown)

As Figure 12 shows riPSC successfully differentiated as confirmed by expression of germ layer specific proteins.

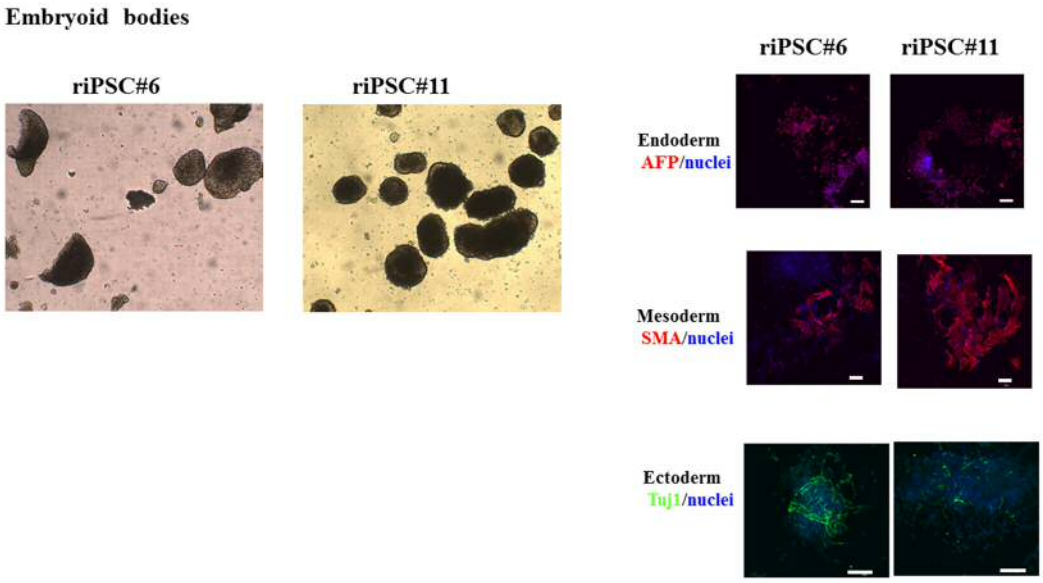

Figure 12.riPSC *in vitro* differentiation. Dissociated riPSC formed embryoid bodies in suspension culture. Embryoid bodies were attached and differentiated into derivatives of three germ layers: α-Feto protein (AFP), Smooth muscle actin (SMA), and βⅢTubulin (Tuj1).

In vivo differentiation

Our next focus was to investigate the behavior of riPSC *in vivo* by performing teratoma assays.

We subcutaneously injected 1×10^6 cells in the neck region of BALB/SCLC-ν/ν mice. Palpable masses developed in all the injected mice. We had set an endpoint for tumor size extraction at 2cm diameter. We observed a difference in tumor mass growth rate, whereby tumor masses from riPSC#3 and riPSC#11 injection grew significantly, more rapidly in comparison to riPSC#6 injected groups. We harvested these masses earlier in accordance to our endpoint. Mice were sacrificed and tumor masses harvested 3-5 weeks after injection. Tumor masses were fixed in 4%PFA and then embedded in paraffin. Sections were cut and H&E staining performed. Tumors from riPSC#6 consisted of derivatives of all three germ layers in Figure 13: Glands and ciliated (endoderm); muscle fiber and cartilage (mesoderm); neural tissue and epidermis (ectoderm). On the other hand riPSC#11 and riPSC#3 derived masses consisted of undifferentiated cells and were identified as immature teratomas.

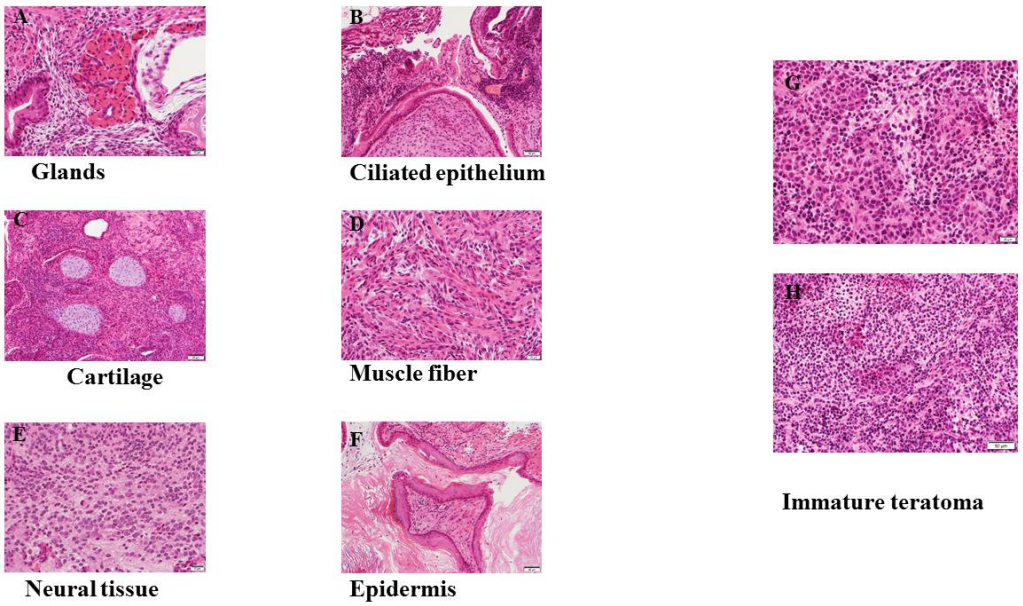

Figure13. riPSC *in vivo* differentiation. Dissociated riPSC were injected into immunocompromised mice. A~F riPSC#6 derived teratoma consisted of endodermal glands and ciliated epithelium, mesodermal cartilage and muscle fiber, ectodermal neural tissues and epidermis. G and H riPSC#11 derived tumor consisting of undifferentiated cells.

Culture system for directed differentiation of riPSC toward a neuronal fate

We first subjected riPSC to a differentiation protocol similar to that of P19 cells involving exposure to retinoic acid (RA). riPSC were dissociated in single cells using trypsin and then grown under floating conditions for 4 days in DMEM/F12 media supplemented with 1%B27 and 0.5μM RA. During this period, spherical aggregates formed. These were trypsinized and replated on pol-l-lysine coated culture dishes. Cells were cultured further for 8 days in DMEM/F12 supplemented with 1%N2, 1%B27 and 0.5μM RA. On day 12 the cells were fixed with 4%PFA and immunostained for the neuron marker βⅢ tubulin. Results are shown in Figure 14. While the cells appeared to be positive for βⅢ tubulin, they had few axonal like projections that are typical of neurons. Moreover, the immunostaining had a high back ground. We attempted to expose riPSC to a modified protocol as well use different antibodies.

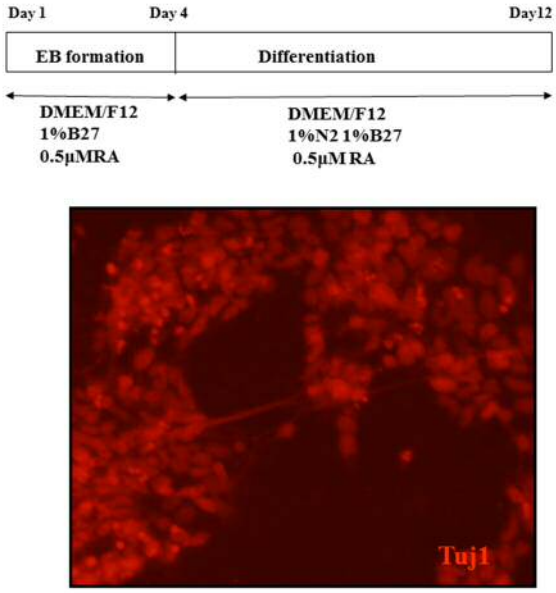

Figure14. Directed differentiation of riPSC toward a neuronal fate. Immunocytochemical analysis of differentiated riPSC at day 12. Cell were positive for the neuronal marker βⅢTubulin (Tuj1) (red).

We modified and applied two protocols that at the time been reported to induce iPSCs to become neural lineage cells (Chang MY *et al*., 2010; Kikuchi T *et al*., 2011). A scheme of the method used is shown in Figure 15. riPSC were dissociated into single cells using Accutase and allowed to form embryoid bodies in riPSC media without LIF and 2i for 7 days. EBs were mildly dissociated using Accutase and replated on gelatin coated dishes for an induction step. Culture media was changed to DMEM/F12 supplemented with 1%B27 and 1%N2. During this culture period, we observed morphological changes and cells acquired bipolar morphology typical of neural stem cells.

We explored the identity of these cells by immunostaining for neural progenitor cell marker Nestin. As in Figure 15.B, we confirmed a large population of nestin positive cells. RT-PCR analysis also showed upregulation of *nestin*, *pax6* and *blbp* in comparison to EB differentiation day 7. Furthermore early neuronal markers *Ascl1, Satb2, Trb1* and *NeuroD1* were also expressed confirming neuronal patterning.

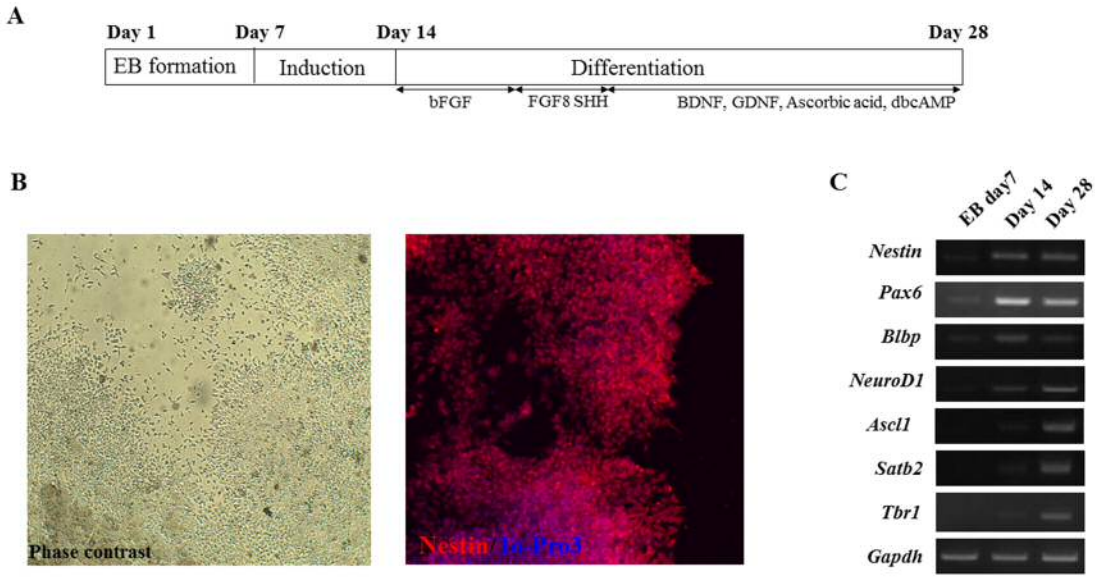

Figure15. Directed differentiation of riPSC toward a neuronal fate. A. Schematic of differentiation protocol. B. Day 14 differentiated riPSC. Cells acquired bipolar morphology and were positive for Nestin (red). Nuclear stain Topro (blue). C. RT-PCR analysis of early neuronal markers at various stages of differentiation.

Having confirmed the specified differentiation had been initiated, we subjected the cells to the last part of the differentiation protocol. For this the cells were replated onto poly-l-lysine coated dishes and exposure to 10ng/mL basic fibroblast growth fator (bFGF) and sonic hedgehog (Shh). After 5 days bFGF and Shh were withdrawn and cells treated with BDNF, GDNF, ascorbic acid and dbAMP for terminal differentiation. After 21 days of differentiation, cells were fixed with 4%PFA and immunostained for neuron marker proteins βⅢ Tubulin and Map2. Results are shown in Figure 16. The cells had acquired morphology typical of neurons and abundantly expressed βⅢ Tubulin and Map2.

We also attempted to characterize the type of neuron population. Differentiation had been

initiated with the mophogen, Shh which is known to direct differentiation to dopaminergic neurons (Cooper O *et al.* 2010; Hartfield EM *et al.* 2014). Therefore we immunostained day28 riPSC derived neurons against tyrosine hydroxylase (TH), a marker for dopaminergic neurons. Neurons were identified as βⅢ tubulin positive cells. We detected TH expressing cells albeit the population being much lower than we had anticipated. We resorted to isolating RNA and conducting RT-PCR analysis for transcripts of other neuron populations. RT-PCR analysis showed expression of dopaminergic genes *TH* and engraild (*EN*)-1 expression as well as N-methyl-D-aspartate receptor (NMDAR) subunits: *GluN1, GluN2A* and *GluN2B*, excitatory amino acid transpoter (*EEAT*)-3 and vesicular glutamate transporter (*VGLUT*)-2 that are typically expressed in excitatory glutamate neurons. We did not detect transcripts for glutamic acid decarboxylase (GAD)-67 (GABAnergic neurons), choline acetyltransferase (ChAT) (cholinergic neurons) or tryptophan hydroxylase (TPH) (serotonergic neurons) (Figure 16). Taken together, these findings indicated that riPSC had indeed differentiated into a neuron population that consisted of excitatory glutamate neurons and dopaminergic neurons.

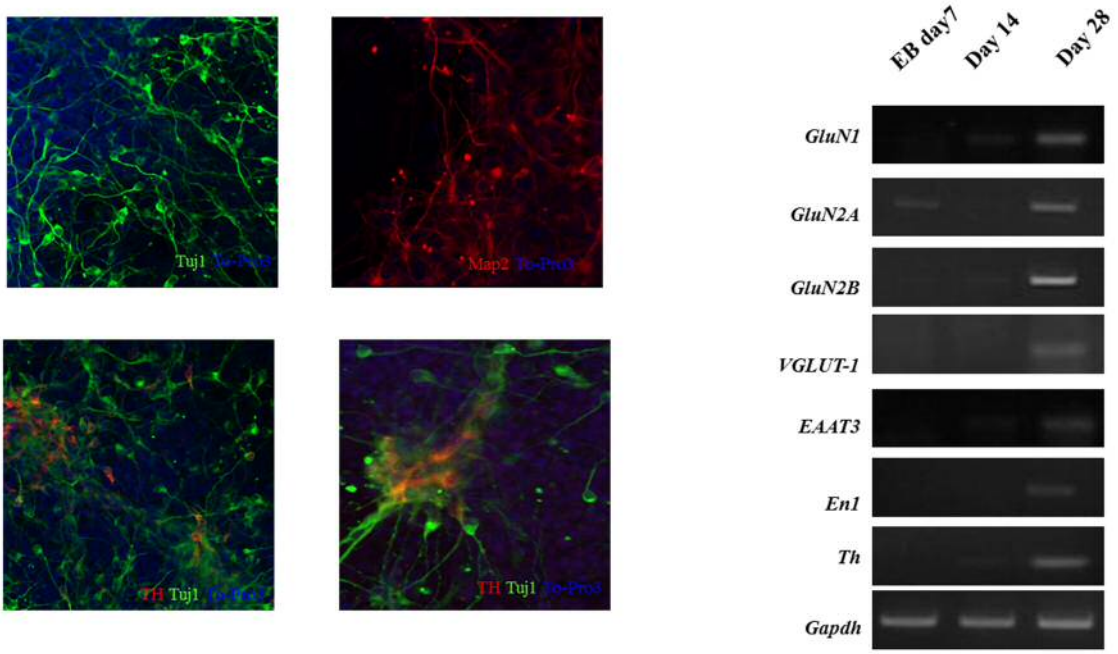

Figure16. Directed differentiation of riPSC toward a neuronal fate. Immunocytochemical analysis of riPSC derived neurons at day 28. Cell were positive for neuronal markers βⅢTubulin (Tuj1) (green) and Map2 (red). A population of tyrosine hydroxylase (TH) (red) cells was detected. RT-PCR analysis of neuron type markers.

Since we had observed differentiated neurons expressed genes typical of NMDA glutamate neurons, we next investigated whether the cells could respond to agonist stimulation. NMDAR stimulation evokes calcium ion infux. We examined calcium signaling following stimulation of differentiated neurons with NMDAR agonist NMDA.

Cell were loaded with Fluo-3-AM at 37 °C , 5%CO_2 for 1 hour. After washing cells were incubated in recording media (Material and methods) for 30 minutes. We then stimulated cells with 200μM NMDA and observed Ca^{2+} transients for 10 minutes. NMDA application lead to an increase in Ca^{2+} levels in the cells. NMDA mediated Ca^{2+} influx was abolished with treatment by

the selective NMDA receptor antagonist,

MK-801. Omission of extracellular Ca^{2+} with 10mM EGTA suppressed response to NMDA indicating the Ca^{2+} dynamics were as a result of Ca^{2+} influx.

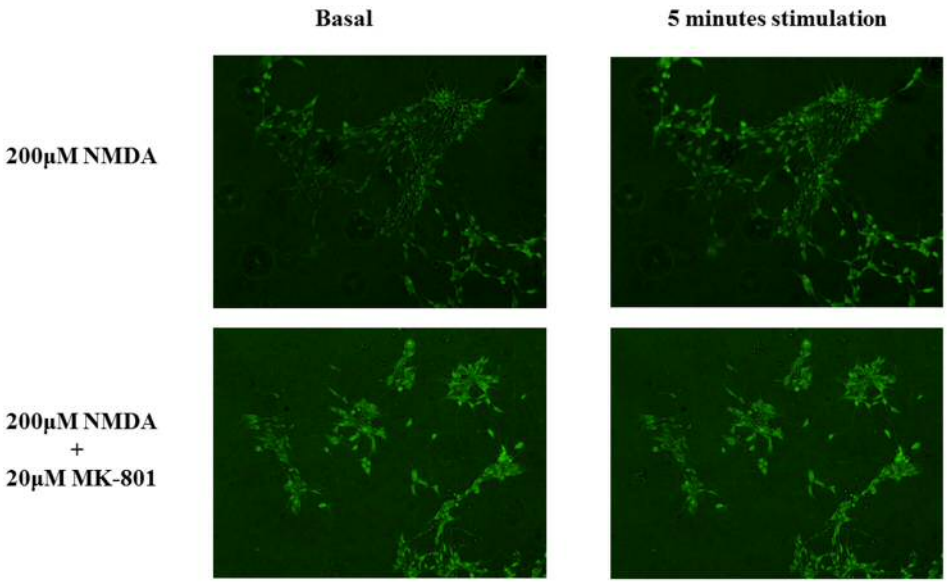

Figure16. Fluo-3-AM Ca^{2+} imaging of day 25 riPSC derived neurons. Basal fluorescence of neurons without stimulation and 5 minutes after stimulation with 200μM NMDA.

These results taken together indicate riPSC can be directed to differentiate into neurons that are reactive to agonist stimulation.

Discussion

We describe generation of iPSC like cells from adult rat fibroblasts using a non viral multiprotein expression plasmid vector. We also characterized the cells with regard to pluripotency markers. riPSC clones differentially expressed the cell surface glycan epitope defined by R-10G antibody but expressed TRA-1-81 epitope similarly. R-10G highly reactive riPSC clone formed teratomas while low reactive clones resulted in tumors consisting of undifferentiated cells. All clones differentiated in a similar fashion *in vitro.* We differentiated riPSC into neurons consisting of glutamatergic and dopaminergic neurons.

Yamanaka and his group established mouse iPS cells using multiple virus vectors and rat iPS cells have been generated using retroviral and lentiviral vectors (Liao J *et al.,* 2009; Li W. *et al*., 2009; Chang Y. *et al*., 2010; Liskovykh M. *et al*., 2011). When we embarked on this work, reports of rat iPSCs were few and the studies used lentiviral transduction to deliver transcription factors (Li W *et al.* 2009; Liao J *et al* 2009; Chang MY *et al* 2010). Viral approach has setbacks including genomic integration and persistence of transduced genes that can be reactivated during differentiation. Indeed, reactivation of c-myc resulted in tumor formation in iPS cell derived offspring (Okita *et al,* 2010). Methods have been developed to generate integration-free iPS cells including episomal vectors (Yu, J. *et al*, 2009), synthesized mRNA (Warren, L. *et al,* 2010), piggy Bac system (Woltjen, K. *et al*, 2009). In this work we successfully delivered a multiprotein expressing non-viral vector through nucleofection. Non-viral technique has only been reported for rat iPS cell generation by Merkl *et al.* (Merkl *et al*, 2013).

At first we cultured generated colonies in riPSC media containing human LIF. Colonies however had rough edges unlike those of previous reports (Li W *et al.* 2009) suggesting LIF alone was insufficient in maintaining these cells in culture. Li *et al.* utilized LIF in combination with chemical inhibitors, CHIR99021 and PD035901 (2iL). Addition of 2i to our culture system

improved colony morphology and colonies acquired clear boundaries. Both rat ESC and rat iPSC studies have shown 2i are necessary for maintaining these cells n culture. 2i block differentiaton pathways by 1) blocking MAPK/ERK pathway 2) reducing GSK3 activity hence maintaining pluripotent state while leading differentiating cells to cell death (Ying *et al.* 2008). iPS cells are susceptible to sporadic differentiation and 2iL system reduces differentiation. Recently, Chen Y. et al reported unsolicited differentiation could be attributed to over inhibition of GSK3 and fine tuning of GSK3 inhibitor concentration increases stem cell maintenance in rat ES cells (Chen Y. *et al,* 2013). It is probable that this is the also the case with rat iPS cells and would be interesting to explore.

Expression of pluripotency makers is paramount in identification and characterization of iPS cells. riPSC we generated expressed Nanog *a*nd SSEA1 proteins as well as various pluripotency marker transcripts. These results are in accordance with reports on rat ES and iPS cells from other groups mentioned above. Moreover, riSPC continued to express Nanog and SSEA-1 after multiple passaging.

Methylation status of *Oct3/4* promoter region were inconsistent with previous reports on rat iPS cells. Merkl *et al*. reported the region as being almost completely hypomethylated. The data discrepancy could be attributed to the type of vector used, difference in species of source cells or as a result of unsuccessful reprogramming. Unsuccessful reprograming is highly unlikely given we detected endogenous Nanog transcript expression as well as protein expression. Alternatively, it could be speculated that the first two demethylated sites in the *Oct3/4* promoter region may be sufficient to express *Oct3/4*. Further studies are needed to clarify which demethylation site(s) are pivotal for *Oct3/4* expression.

Karyotypic abnormalities occur frequently in ES and iPS cells. Chromosomal instability is widely reported in mouse and human iPS cells (Laurent LC *et al.* 2011). Liskovykh *et al*.

reported high ratio of aneuploid and tetraploid cells in rat iPS cells they had generated. Our findings are in accord with this. Rate of karyotypic abnormalities is known to increase with increasing passages and culture duration. Prolonged passaging and growth in culture results to gain of chromosomes. Abnormalities may also occur during reprogramming process (Ben-David U and Benvisity N. 2011). Aneuploidy results in alteration in gene expression as well as alterations in cellular function and processes.

We characterized riPSC with regard to a keratan sulfate glycan epitope defined by R-10G antibody. We observed unexpected differential expression of R-10G binding epitope while TRA-1-81 binding was similar.We had first aimed at exploring usefulness of R-10G as a new marker identifying rat iPS cells. Preliminary work in developing the antibody showed the antibody reacted with human ES and iPS cell lines. Although riPSC reacted with R-10G, it was surprising that aneuploidy clones had lower reactivity in comparison to normal karyotype clone. R-10G and TRA-1-81 epitopes are both keratan sulfate glycans, albeit of different structure, and share the carrier protein, podocalyxin (Kawabe K. *et al* 2013). It could be speculated that the difference in R-10G binding was as a result of a difference in carrier protein level expression rather than expression of R-10G binding epitope in riPSC clones. However this notion is improbable considering TRA-1-81 expression was comparable.Cell surface glycans are popular targets for not only identifying and characterizing pluripotent stem cells but also for exploring pluripotency, selfrenewal and differentiation. Glycan signatures vary with development stages and differentiation states. They are also distinct in cells types (Tateno H. *et al.,* 2011). The reprogramming process is basically de-differentiation of somatic cells to a pluripotency after which cells express pluripotency markers that were initially unexpressed. In this light, it is probable that a sort of shift/alteration in glycan surface molecules occurs as cells acquire pluripotency. Indeed, somatic cells originally with distinct glycan profiles acquire glycan profiles

similar to ES cells upon induction to pluripotency (Tateno H. *et al*., 2011; Hasehira K. *et al .,* 2012).

In summary, we identified a unique glycophenotypic variation in riPSC clones. The correlation between karyotypic anomaly and observations on R10-G binding are also of great interest and remain to be elucidated. Out of the 11 clones that we picked and expanded, only three had been successfully maintained in culture. This limited the number of clones we analyzed. Analysis of more clones, especially those of normal karyotype to further draw clear conclusions on the observations is necessary.

We explored differentiation potential of riPSC. We applied EB formation system accompanied by mono layer culture. In vitro differentiation of ES and iPS cells is normally initiated though EB formation during which stem cell state is lost and differentiation initiated. Further culture of EBs in adherent conditions enables cells to differentiate and mature. riPSC were able to form EBs which differentiated into endoderm (AFP positive), mesoderm (SMA) and ectoderm (βⅢ Tubulin) lineages. This is in accordance with previous studies on rat ES and iPS cells.

In our system suspension culture of riPSC was carried out iPS media (containing 15% FBS) without 2iL resulting in aggregate formation. This was in disagreement with Merkl et al. who also generated rat iPS cells using a non viral vector. They reported rat iPS cells cultured in suspension in medium containing serum died after two days and did not form EBs. Their system additionally required GSK3βinhibition for successful EB formation (Merkl et al. 2013). However, our findings are in agreement with Chang et al who generated EBs from rat iPS cells in serum containing media similar to ours (Chang MY et al, 2010). These observations suggest that fine differences in nature of rat iPS cell lines exist that may in turn affect optimal culture conditions and processes. riPSC clones not only formed EBs similarly but also differentiated into three germ layers derivatives. We did not observe any differences that could distinguish clones during

differentiation culture.

riPSC could form tumor masses when injected into immunocompromised mice. Tumor masses from R-10G highly reactive clones were identified as teratomas. riPSC clones with low reactivity to R-10G formed tumors made up of undifferentiated cells. Teratoma assay is considered a gold standard to analyze pluripotency of pluripotent cells especially during establishment of new cell lines (Gertow *et al*. 2007; Wesselschmidt 2011). Teratomas are benign tumors made up of differentiated cells from all three germ layers. The assay involves injection of cells into immune-compromised mice, whereby they proliferate and differentiate forming tumors. Tumors are extracted and subjected to histopathological analysis to verify nature of the cells comprising the tumor. Pluripotency and tumorigenecity are closely related phenomena (Knoepfter, 2009; Andrew S. Lee *et al*, 2013). In this light, teratoma assay serves as a potent test not only for pluripotency but also a test for tumorigenecity.

riPSC#6 resulted in teratomas consisting of cells of all three germ layers confirming trilineage commitment *in vivo*. Tumors formed by clones with low R-10G reactivity had more rapid growth and were harvested earlier. The aggressive growth rate couple with the poorly differentiated nature is suggestive of a tumorigenic nature although further analysis are necessary to elucidate this possibility. The reason of these clones did not form mature teratomas is unclear. However, karyotypic abnormality can be speculated.

As previously discussed, R-10G reacts to human ES and iPS cells with almost no reactivity to human EC cell lines. EC cells are tumorigenic and result in malignancies. In this light, it is reasonable to consider that a difference in R-10G glycan epitope profile of teratoma and non-teratoma forming riPSC exists. Fujitani et al. in their work reported cellular glycomes to be highly cell type specific and suggested the presence of stem-cell specific glycosylation spectra (Fujitani N. *et al* 2013). Epitopes defined by R-10G could provide a useful tool to investigate

glycan dynamics surrounding pluripotency and tumor formation.

We also determined riPSC could be directed to differentiate into neural lineage cells. riPSC underwent a step wise acquisition of neuropotency, morphological changes and expressed markers for observed in authentic neural progenitors and neurons. Chang et al. reported derivation of neurons from rat iPS cells (Chang MY *et al* .,2010). In this study 10% of neuron population was identified as dopaminergic. However, the remaining population was no defined. We identified excitatory glutamatergic neurons alongside a population of dopaminergic neurons. Other neuronal types were not identified, by RT-PCR at least. Although differentiation was done using morphogens, Shh and FGF-8, which drive dopaminergic neuron differentiation, only a small population of $TH^+/Tuj1^+$ cells was detected. Neural differentiation using same morphogens on human iPS cells yield about 80% TH positive neurons (Kikuchi T. *et al*, 2011). This suggests a difference in response to morphogenic stimulation in rat and human iPS cells. Neurons differentiated from riPSC could be used to study pharmacological glutamate neurotransmitter signaling.

In summary, we demonstrated that iPS cells can be generated from adult rat fibroblasts using a non viral plasmid vector. riPSC generated have ES cell morphology and expresses pluripotency markers. Expression of a keratan sulfate glycan epitope defined by R-10G antibody varied in riPSC clones. Teratoma formation assay showed a clone highly reactive to R-10G formed teratomas while low reactive clones results in tumors consisting of undifferentiated cells. This glycophenotypic difference may potentially be useful in evaluating rat iPS cells as well as studying the role of glycans in pluripotnecy and carcinogenesis. riPSC could be differentiated into a neuronal lineage that can be applied in the study of neurogenesis and neuron functions.

PART 2: **Selective HDAC8 inhibition in pluripotent P19 cells.**

INTRODUCTION

Histone acetylation and deacetylation are epigenetic processes that regulate gene expression and in turn cellular functions (Shahbazian MD and Grunstein M, 2007; Haberland M. *et al.,*2009). Histone acetyl tranferases (HATs) transfer acetyl groups to lysine residues on histones causing chromatin structure to relax due to reduced interaction of DNA and histones. Histone deacetylases (HDACs) are a group of enzymes that are responsible for deacetylation of lysine residues on histones and non-histone proteins. Deacetylation of histones alters chromatin structure thus regulating downstream gene expression and in turn various other cellular processes. HDAC isoforms are classified into four classes; Class I (HDAC 1,2,3 and 8) which are homologous to yeast RPD3, Class Ⅱ (HDAC4-7,9and10) which are homologous to yeast Hda1 , ClassⅢ(Sirt1-7) and ClassⅣ(HDAC11) (de Ruijter AJ. *et al.,* 2003; Gregoretti IV *et al.,* 2004). HDAC inhibition has extensively been reported to suppress proliferation and alter differentiation in tumor cells. Indeed, HDAC inhibitors (HDACi) are clinically used in cancer management (vorinostat). Application of HDACi in nonmalignant diseases is also of interest. Disconcerted acetylation homeostasis alongside increase in HDAC activity in neurodegenerative disorders is widely reported (Saha RN. *et al.,* 2006; Kwok JB. 2010) and HDAC inhibition has been shown to mediate neurogenerative and neuroprotective properties in neurological conditions such Alzheimer's disease, Huntington's disease, stroke and Parkinson's disease (Fischer A *et al.,* 2007; Chuang DM. *et al*. 2009). However, reports on effects of HDAC inhibition in the brain and in neurodegenerative conditions are contradictory. Individual HDAC isoforms function neuroprotectively alleviating neurological conditions (Mac C.*et al.,* 2011) or result in neurotoxicity (Bardai FH. *et al.,* 2011). Intriguingly, some HDAC isoforms function in a differential manner exerting both protective and toxic effects (Bardai FH. *et al.,* 2012). This

contraction could be attributed to the non-selectivity nature of the inhibitors used as majority of HDACi available are poorly selective and target multiple HDAC isoforms. Therefore studies using isoform-selective inhibitors should be useful in understanding contribution of individual HDAC isoforms in the nervous system as well as providing potential therapeutic agents devoid of undesirable effects.

Additionally, there are reports showing epigenetic modification via HDAC inhibition improves reprogramming efficiency and promote iPS cell generation (Huangfu D. *et al.,* 2008; Mali P. *et al.,* 2010). In this light, HDACi can be useful in modulating differentiation processes.

HDAC8 is a unique member of the class 1 HDACs. HDAC8 shares only 43% sequence identity with other members of its class as well as a shorter C terminal (Buggy JJ *et al.,* 2000; Bolden JE *et al.,*2006). Moreover, HDAC8 has a unique expression pattern and is abundantly expressed in the brain, kidney and prostate (Hu E *et al,.*2000). HDAC8 has been implicated in with a number of diseases including neuroblastoma (Oehme I *et al.,*2009) and Cornelia de Lange syndrome (Deardorff MA *et al*., 2012). Importance of HDAC8 is mostly associated with tumor cell proliferation and its knock down inhibits growth (Hu E *et al,.*2000). However, little is known about the role of HDAC8 during development and differentiation.

HDAC8 high expression in neuroblastoma and its association with poor prognosis (Oehme I *et al.,*2009) lead us to hypothesize that HDAC8 inhibition might regulate neurogenesis. In this study, we investigated involvement of HDAC8 inhibition on embryonic neurogenesis using retinoic acid treated P19 cells as a model for neural progenitor cells and a HDAC8 selective inhibitor (Suzuki T. *et al*. 2012). P19 cells are pluripotent cells that can be induced to differentiate to various cells by aggregation and induction by drugs. P19 cells induced with retinoic acid (RA) under floating culture conditions form embryoid body like aggregates that differentiate into neural lineage cells (Mc Burney MW. e*t al.,* 1983).

RESULTS

Class1 HDAC isoform expression in RA treated P19 cells

Firstly, we examined the expression of the Class1 HDACs HDAC 1, 2, 3, and 8 in undifferentiated and RA treated P19 cells. As shown in Figure 1, all Class 1 HDACs were uniformly expressed in P19 cells before and after induction with RA.

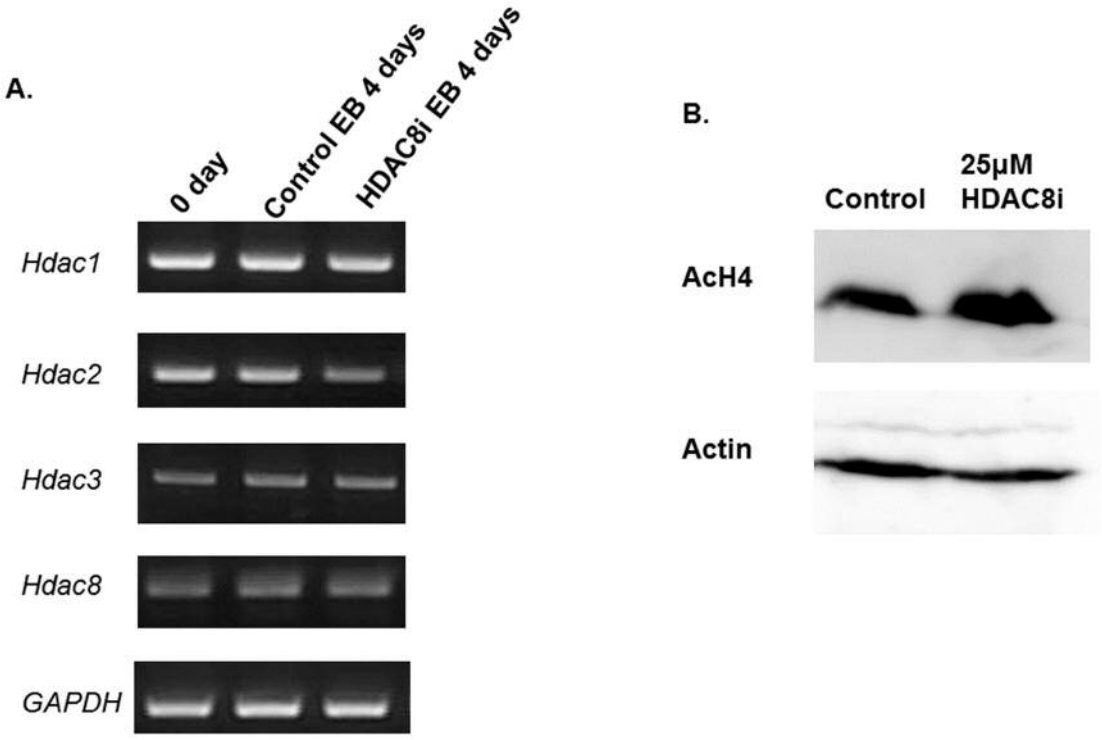

Figure 1. A. Expression of class Ⅰ HDAC isoforms. P19 cells treated with RA in non-adherent conditions for 4 days. RT-PCR analysis of 0 day, day4 control and HDAC8i treated embryoid bodies (EB). B. Histone4 acetylation. Western blot analysis of P19 cells treated with RA in non-adherent conditions for 48 hours treated HDAC8i. Actin is loading control.

Next, we investigated whether histone 4 (H4) acetylation level was modulated by HDAC8 inhibition. Cells were treated with vehicle (DMSO) or 25μM HDAC8 inhibitor for 48 hours and

protein samples collected. Western blotting results showed an increase in acetylated Histone 4 (AcH4) levels in inhibitor treated cells in comparison to control (Figure 1B).

HDAC8 inhibition decreases size of RA treated P19 cell aggregates

It has been widely reported that pan-HDAC inhibitors such as the aliphatic acids, valproic acid (VPA) and sodium butyrate; hydoxamates, vorinostat (SAHA) and trichostatin A (TSA) result in cell cycle arrest, decrease in proliferation and induce apoptosis in a cell specific manner (Dokmanovic M. *et al.,* 2007). We investigated the effect of HDAC8 specific inhibition on proliferation and cell survival of RA treated P19 cells. P19 cells cultured in non-adherent conditions form round clustered aggregates consisting of proliferating cells.

P19 cells were treated with RA with and without HDAC8 inhibitor at various concentrations. HDAC8 inhibition resulted in distinct reduced aggregate formation in a dose dependent manner (Figure.2A). At 10μM HDAC8i, we observed both large and small aggregates while at higher concentrations small aggregates were most apparent. Quantitative analysis of total aggregate area was conducted and results were shown in Figure 2B. Difference in cell proliferation was further evaluated via measurement of 2-(2-methoxy-4-nitrophenyl)-3-(4-nitrophenyl)-5-(2,4-disulfophenyl)-2H-tetrazolium (WST-8) reducing activity. WST-8 reducing activity was lower in HDAC8i treated cells in comparison with control (Figure.2C).

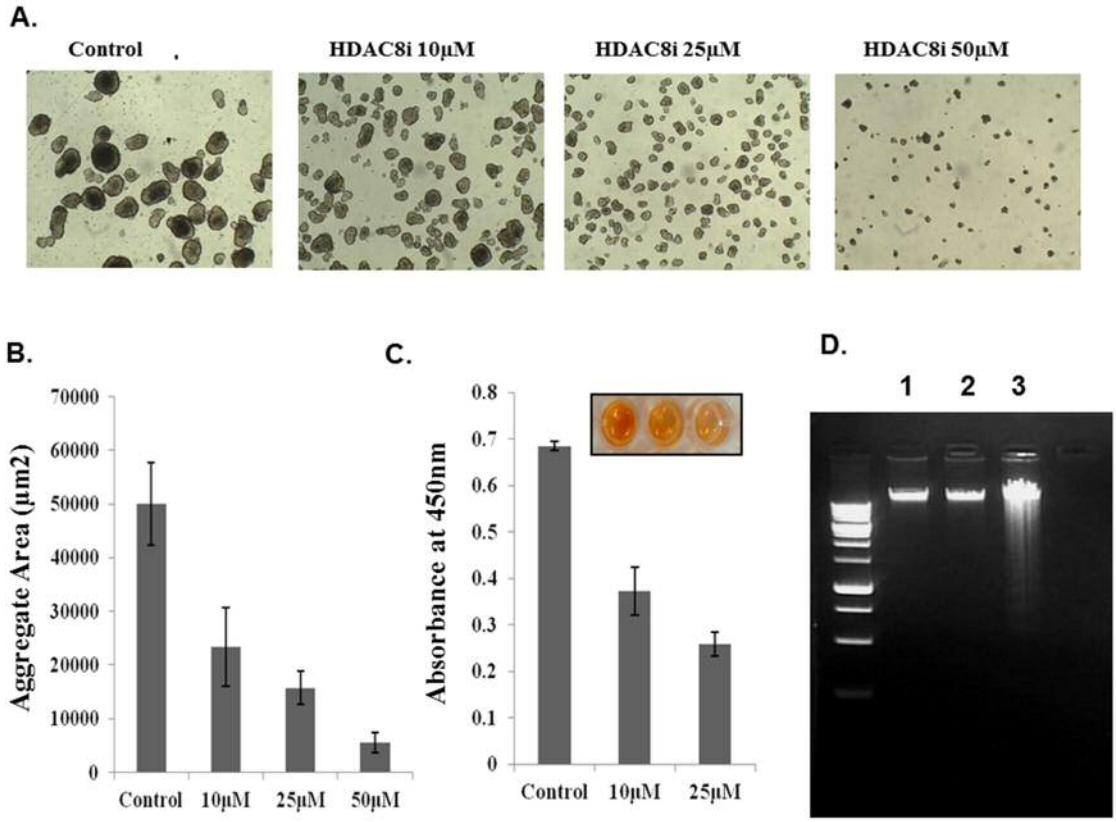

Figure 2. Concentration dependent suppression of proliferation by HDAC8 inhibition. P19 cells treated with HDAC8i in the presence of RA in non-adherent conditions for 4 days. A. Phase contrast images of aggregates. B. Area of aggregates at culture day 4. C. Cell viability determined by WST-8 assay. D. DNA fragmentation analysis. Lane 1: Control, Lane 2: HDAC8i 25 μ M, Lane3: RA 100 μ M as DNA fragmentation positive control.

HDAC inhibition has been reported to induce apoptosis (Tang X. *et al.,* 2004). It could be postulated that HDAC8i treatment reduced aggregate size as a result of a toxic effect that in turn resulted in increase of cell death. Consequently, we evaluated the extent of cell death in control and HDAC8i treated cells. Cell death was evaluated via analysis of DNA fragmentation in genomic DNA isolated from aggregates after 4 days of culture. No significant difference in DNA fragmentation was seen between untreated and HDAC8i treated cells (Figure 2D). Collectively, these results demonstrate HDAC8 inhibition reduces cell proliferation without inducing apoptotic cell death in RA induced P19 aggregates.

Expression changes in cell cycle related and neural differentiation specific genes after HDAC8i treatment

In the light of the proliferation suppressing effects observed, we sort to elucidate on the effect of HDAC8 inhibition on expression of cell cycle associated genes. RT-PCR analysis showed an up regulation of cyclin dependent kinase inhibitor 1A (p21) mRNA expression in HDAC8i treated cells. On the other hand, HDAC8 inhibition did not result in significant differences cyclin D1 and Ki67 mRNA expression levels. We also examined transcription of *Musashi-1* which contributes to maintenance of neural precursor cells and is a marker of these cells. RT-PCR analysis showed HDAC8 inhibition induced a reduction of *Musashi-1* expression. Constant with this finding, protein level of Sox2 which functions to maintain neural precursor cells in their progenitor state,

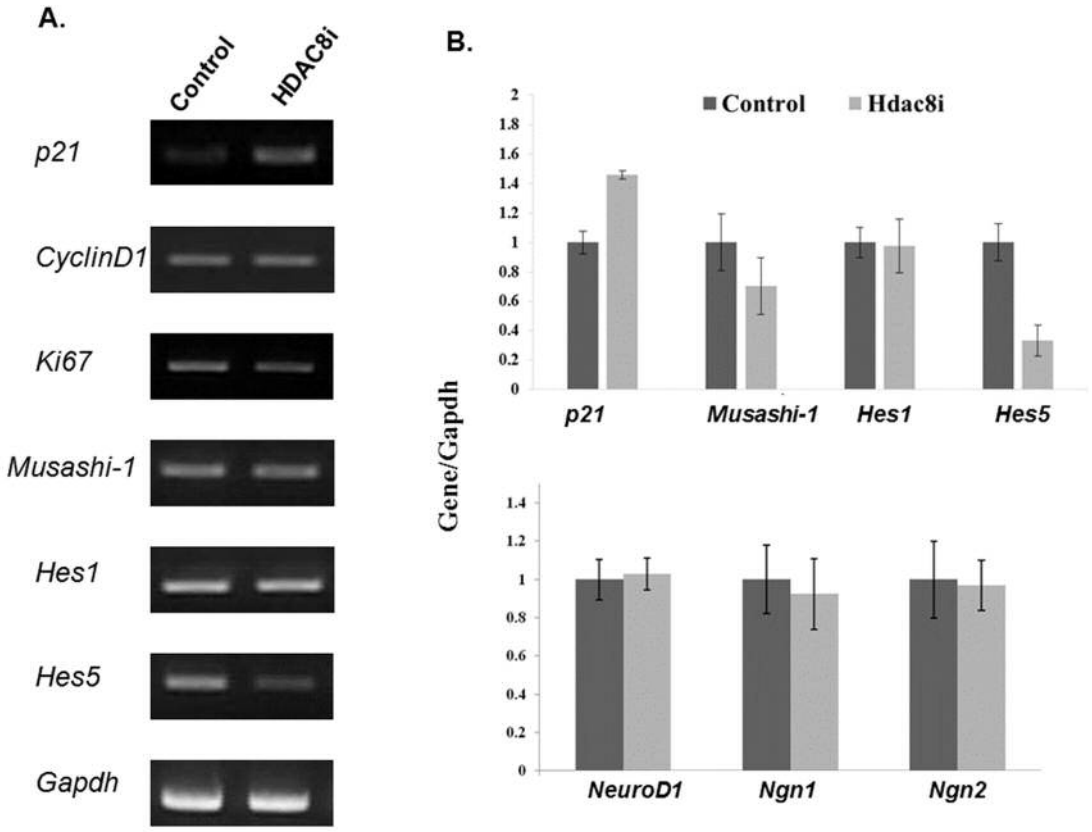

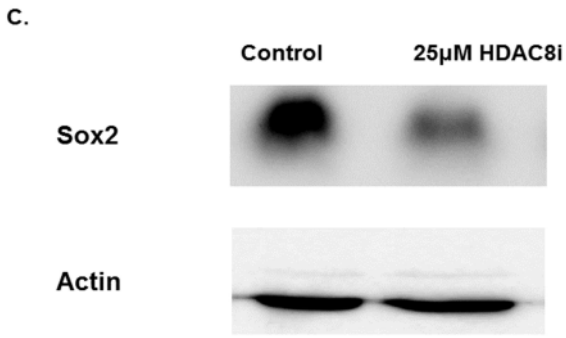

Figure 3. Expression of cell cycle regulators, pluripotency markers and bHLH factors. P19 cells treated with HDAC8i in the presence of RA in non-adherent conditions for 4 days. mRNA and protein were isolated at day 4. A. RT-PCR analysis for mRNA expression. B. Quantitative data of RT-PCR results (mean of 4 independent experiments). C. Western blot analysis for Sox2. Actin is loading control.

was decreased in inhibitor treated cells (Figure.3C). Thus taken together, these data suggest HDAC8 inhibition suppresses cell proliferation and undifferentiated state of RA treated P19 cells.

During the process of neurogenesis, self-renewal of progenitor cells and the switch to neuronal differentiation is controlled by the balance in 1) expression of repressor bHLH factors such as Hes1 and Hes5, which regulate and maintain undifferentiated state, and 2) proneural bHLH factors such as Math, Ascl1, NeuroD, which positively promote cell cycle exit for differentiation. Self-renewing NPCs convert into mitotically inactive cells that later differentiate into mature neuronal lineage cells including neurons, astrocytes and oligodendrocytes. Given that HDAC8 inhibition exerted an anti-mitotic effect associated with a decrease in factors contributing to maintaince of progenitor state, we sort to investigate whether expression of bHLH factors was

affected. RT-PCR analysis showed a decrease in expression of the repressor bHLH factor, Hes 5 following HDAC8 inhibition. Contrastingly, Hes 1 mRNA expression levels was not changed. Given cell-cycle exit is coupled with initiation of differentiation, we analyzed whether HDAC8 inhibition during proliferation would affect expression of proneural bHLH factors. Expression of Neuorogenin1 (Ngn 1), Neurogenin 2 (Ngn 2), NeuroD1 were assessed by real-time PCR. We did not observe any significant alterations in transcript expressions of these genes (Figure 3B).

DISCUSSION

HDAC8 remains the least studied class Ⅰ isoform in regard to neurogenesis and neurodegenerative conditions. We used RA treated P19 cells, a well-established model of neural precursor cells, to investigate effect of HDAC8 specific inhibition during neurogenesis. Firstly, treatment with HDAC8i resulted in robust inhibition of cell proliferation without causing cell death. Inhibition of cell proliferation was characterized by upregulation of *p21* expression. Increase of *p21* expression is associated with cell cycle arrest in G1 phase (Ocker M.*et al.,*2007). In this light, inhibition of cell proliferation we observed could be attributed to cell cycle arrest in G1 phase, at least in part. As we only analyzed cyclin D1 transcript expression, which was unaffected by HDAC8 inhibition. Further analysis of other cyclins is needed evaluate their possible involvement.

Secondly, our findings demonstrate HDAC8i treatment resulted in decrease in Sox2 protein levels. Sox2 is involved in maintenance of progenitor state in neural precursor cells. Effect of HDAC inhibition on Sox2 expression appears to vary in cell types. Zhou Q. *et al.* reported broad class Ⅰ and class Ⅱ HDAC inhibitors down regulated Sox2 expression in adult mouse neural stem cells (Zhou Q. *et al.* 2011). Contrastingly, Sox2 was negatively regulated by HDAC2 in experiments using conditional gene deleted neuroblasts (Jawerka M. *et al.,*2010). In oligodendrocyte precursor cells, inhibition of HDAC activity upregulated genes that maintain neural stem cell state including Sox2 (Lyssiotis CA. *et al.,* 2007). HDAC regulation of Sox2 expression is probably cell type specific and dependent on the HDAC isoform inhibited.

We also found that HDAC8 inhibition downregulated *Musashi-1* expression. This is in agreement with our data showing downregulation of Sox2 as Musashi-1 functions to maintain undifferentiated state of neural progenitor cells. Musashi-1 is an RNA-binding protein associated

with maintenance and cell division of neural progenitor cells (Okano H. *et al.,*2005). Furthermore, Musashi-1 is a translational repressor of p21 and regulates the Notch-1 signaling pathway that in turn alters cell cycle progression (Okano H. *et al.,*2005). Consistent with our findings, Oehma I. *et al.* reported down regulation of nestin (a marker for neural progenitor cells) in HDAC8 knock down neuroblastoma cells (Oehma I. *et al.*, 2009). Taken together findings suggest HDAC8 inhibition is involved in suppression of progenitor and undifferentiated state.

Furthermore, we observed suppression of the repressor bHLH factor Hes5 mRNA expression. However, *Hes1* and proneural bHLH factors examined were not altered by HDAC8 inhibition. Hes factors are effectors for notch signaling pathway and functionally antagonize proneural bHLH genes including Mash1, Math1 and Neurogenin hence preventing differentiation (Ohtsuka T. *et al.,* 2001; Kageyama R *et al.*2005). Notch signaling plays an important role in neural development, cell proliferation and differentiation (Miele and Osborne, 1999; Kageyama R *et al.*2008). Notch mediated cell-cell interaction is essential for maintenance of dividing cells and its activation inhibits cellular differentiation. Hes5 downregulation could be speculated to be as a result of epigenetic modulation of complexes as the promoter or because of alteration of Notch signaling pathway by other genes such as *Sox2* and *Musashi-1*. Tiberi L. *et al.* reported epigenetic silencing of Hes5 through the recruitment of the NAD^+ - dependent deacetylase, Sirt1, to Hes5 promoter (Tiberi L. *et al.*, 2012). Although, of a different type, this study suggests regulation of Hes5 expression through epigenetic mechanisms.

As previously described, downregulation of repressor bHLH factors is concomitant with proneural bHLH factor activation driving differentiation. *NeuroD1, Ngn1* and *Ngn2* were unaffected by HDAC8 inhibition. However, we did not exhaustively analyze proneural bHLH factors and it is not possible to draw conclusions on whether HDAC8 inhibition effect on proneural genes from the present data. Valproic acid (VPA) a pan-inhibitor, has been reported to

up-regulate NeuroD1 in adult neural progenitor cells (Hsieh J. *et al.,*2004). In contrast to this, Yu IT. *et al.* reported up-regulation of Ngn1 and Math1 but not NeuroD1 following VPA treatment in embryonic neural progenitor cells (Yu IT. *et al.* 2009). Broad class I and Ⅱ HDAC inhibitors suberoylanilide hydroxamic acid (SAHA) and sodium butyrate (NaB) upregulated NeuroD1 and Ngn1 in adult subventricular cells (Zhou Q. *et al.,* 2011). This implies HDAC inhibition indeed upregulates proneural bHLH factors. However, certain differences in molecular mechanism responses such as cell type may exist.

In summary, HDAC8 specific inhibition reduced proliferation in undifferentiated RA induced P19 cells. Restriction of proliferation was characterized by gene and protein expression changes demonstrating G1 arrest concomitant with suppression of undifferentiated progenitor state.

Mechanisms through which HDAC8 inhibition is resulted in our observations, the causal steps and precise order of events leading to alterations in proliferation are crucial points that need to be determined through further studies. HDAC8 inhibition could alter expression of genes that mediate notch signaling such as Sox2 and Musashi-1, impacting downstream regulatory systems. Alternatively, HDAC8 inhibition may directly regulate Hes5 transcription. Chromatin immunoprecipitation (ChiP) and promoter assays on the Hes5 promoter should elucidate on this.

CONCLUSION

In part 1, we generated rat iPS cells using a non-viral plasmid vector. The cells expressed hallmark pluripotency marker mRNA and proteins and differentiated to cells of three germ layer *in vitro*. We found a difference in glycophenotype among riPSC with regard to keratan sulfate glycan epitope that binds R-10G antibody. riPSC clone highly reactive to R-10G formed teratomas consisting of derivatives from three germ layers. Clones with low reactivity formed tumor masses made up of undifferentiated cells. This difference in glycophenotype could be useful to evaluate and study the role of glycans in pluripotency and tumorigenesis. riPSC were also differentiated to neurons using a multistep protocol and resulting cells consisted of glutamatergic and dopaminergic neurons. Glutamatergic neurons responded to agonist stimulation. riPSC can serve as a source for neurons for pharmacological and toxicological studies as well as a model to study neurogenesis process.

In part 2, we explored the effect of HDAC8 inhibition on neurogenesis using P19 cells a model. HDAC8 was expressed in retinoic acid induced P19 cells and inhibition suppressed proliferation without inducing cell death. Upregulation of *p21* suggests G1 cell cycle arrest. We found HDAC8 inhibition resulted in decrease in Sox2 protein, Musashi-1 and Hes5 mRNA expressions implying a change in undifferentiated state. The findings in this part of the thesis uncover as well as suggest a role for HDAC8 inhibition in neurogenesis.

Materials and Methods

Animal experimental procedures were carried out in accordance with the guidelines and laws of the Japanese government and were approved by the Animal Care Committee of Ritsumeikan University.

Cell culture

6 week male wistar rats were sacrificed ethically. Abdomens were sterilized and excess hairs shaved off. Skin specimens were dissected and washed twice in phosphate buffered saline (PBS). Skin specimens were grown on tissue culture dishes in Fibroblast media (Dulbecco's Modified Eagle's Medium (DMEM), supplemented with 10% fetal bovine serum (FBS), 100U/mL penicillin, 100μg/mL streptomycin). Skin specimens were removed after 7 days and cells that migrated out of the skin pieces grown to confluence. Fibroblasts were passaged and used for reprogramming between passage 2 and 4.

Mouse Embryonic Fibroblasts (MEFs) were maintained in Fibroblast media. For feeder layer preparation, MEFs were grown to confluence and inactivated by incubation with mitomycin C at 37°C ·5%CO_2 for 3hours. MEFs were washed thrice with PBS and used for iPSC culture.

rat iPS cells (riPSC) were cultured in riPSC media: high Glucose DMEM supplemented with 15% FBS, 1mM β-mercapto-ethanol, 1× nonessential amino acids , 100U/mL penicillin, 100μg/mL streptomycin, 1000U/mL leukemia inhibitory factor (LIF) supplemented with signal inhibitors 2i including MEK1/2 inhibitor PD 0325901 (0.5μM) and GSK3β inhibitor CHIR99021

(3μM) on inactivated MEFs. Media was renewed daily. Subsequent passage was done using trypsin-based dissociation with a split ratio of 1:4 every 4 to 5 days.

Reprogramming

Reprogramming was conducted using pCAG2LMKOSimO vector (kindly donated by Dr. K. Kaji, University of Edinburgh). 8μg of pCAG2LMKOSimOvector was introduced into 10^6 fibroblasts with the Basic Nucleofector Kit for Primary Mammalian Fibroblasts using the Nucleofector Ⅱ(Lonza) device (program V-013) and plated on inactivated MEFs. Cells were maintained in riPSC media. 400μg/mL G418 was added for selection. Colonies were visible from day 7 post nucleofection and were picked at day 14-20. Individual colonies were transferred to 96 well plates and dissociated with 30μL trypsin. 70μL riPSC media was added and cells transferred to 24 well plates with MEF feeder layer. Colonies were subsequently expanded.

.

In vitro differentiation of riPS

riPSC were dissociated with 0.25% trypsin/EDTA and transferred to non-adherent bacterial culture dishes in riPSC media without LIF and 2i for embryoid body (EB) formation. On day7, EBs were dissociated with Accutase, attached on gelatin-coated tissue culture dishes and maintained in fibroblast media for an additional 7 days. Media was renewed every 2 days.

Differentiation of riPS into Neurons

riPSC colonies were dissociated and plated on non-adherent bacterial culture dishes in riPS

media without LIF and 2i with media change every 3 days. After 7 days EBs were collected by centrifugation and dissociated with Accutase. For induction of differentiation toward neuronal lineage, cells were plated on gelatin-coated tissue culture dishes and maintained in Induction media: DMEM-F12 supplemented with 100U/mL penicillin, 100µg/mL streptomycin, 1% N2 and 1% B27. At culture day 7 cells were dissociated using Accutase and plated on poly-l-lysine coated dishes in Induction media containing 10ng/mL basic fibroblast growth factor (bFGF) and cultured for an additional 5 days after which 100ng/mL FGF8 and 200ng/mL Sonic Hedgehog (SHH) were added. Media was changed to Induction media supplemented with 2% B27, 30ng/mL brain derived neurotrophic factor (BDNF), 50ng/mL glia derived neurotrophic factor (GDNF) and 200nM ascorbic acid for terminal differentiation.

Alkaline phosphatase staining and immunocytochemistry

Alkaline phosphatase staining was performed using the Alkaline Phosphatase Detection Kit (Millipore, USA) according to the manufacturer's recommendation.

For immunocytochemistry, cells were fixed using 4% paraformaldehyde for 15 minutes at room temperature. Cells were then washed with PBS followed by permeabilization with 0.2% Triton X-100 in PBS for 15 minutes at room temperature. For R-10G immunocytochemical analysis cells were not treated with Triton X-100. Blocking was done with 3% FBS for 1 hour at room temperature. Primary antibody reactions were done overnight at 4°C. After washing with PBS, the cells were incubated with the respective secondary antibodies for one hour at room temperature. Cell nuclei were stained using ToPro 3 or DAPI. Cells were imaged with the confocal or fluorescence microscopes.

Primary antibodies used: Nanog (1:500, Abcam), SSEA1 (1:500, Abcam), R-10G (1:100), Nestin

(1:500, Sigma), Smooth actin muscle SMA (1:250), Albumin (1: 250), Class Ⅲβ- Tubulin (1:1000, Millipore), Map2 (1:1000 Sigma), Alexa fluorophores 488 and 555 were used for the respective primary antibodies at 1000 times dilution.

Reverse Transcription-Polymerase Chain Reaction

Total RNA was extracted using Sepazol and treated with DNase I to remove genomic DNA. 1μg RNA was used for cDNA generation using the SuperScript ⅢFirst-Strand Synthesis System for RT-PCR as per the manufacturer's protocol. PCR was performed using Onetaq DNA polymerase. PCR primers used are shown on Table 1. PCR products were resolved on 1.5% agarose gels and visualized by ethidium bromide staining.

Genes	Forward	Reverse
Nanog	aagcagaagatgcggactgt	aggccgttgctagtcttcaa
Oct3/4	cgaggcctttccctctgttcct	tctctttgtctacctcccttccttgc
Sox2	ggccattaacggcacactgcc	ttactctcctcttttgcacccctc
Eras	gctgcccctcagccgactgctact	cactgccttgtactccggtagctg
Lin28	cgggaggaggaagaagagatccac	ccactctgcggattgatgcct
Lefty	tgaccatcaggtggccatttctg	tgttgggcaggctgaccacttg
Fgf4	tgtggtgagcatcttcggagtgg	ccttcttggtccgcccgttctta
Nodal	gagcgtgtttggatggagagg	atgccaacactttcctgcttgac
Esg1	tccagaagtattccaggtcca	ctccagggtcttcatggatt
Nestin	agccattgtggtctactga	tgcaactctgccttatcc
Ascl1	acccccttagccagaggaa	gctgggtgtctggtttgttt

Satb2	tcttctgtgtggtggagcag	ggggcgtctgtcacataact
NeuroD1	acagctcccatgtcttccac	aagattgatccgtggctttg
Pax6	agttcttcgcaacctggcta	ttgagcctcatccggagtctt
Blbp	ccagctgggagaagagtttg	taacagcgaacagcaacgac
Tbr1	gatgctcccttgttgttggt	tcccaatcactggaggtttc
VGluT1	tactggagaagcggcaggaagg	ccagaaaaagcaatgtatgagg
EAAT3	caaaatcgtgggcctgtact	cccagcgattaggaacaaaa
GluN1	ctcatctctagccaggtcta	tcgcatcatctcaaaccagac
GluN2A	actccacactgcccatgaac	ttgttccccaagagtttgctt
GluN2B	gtttgatgaaatcgagctggc	tccagttcctgcagggagtt
En 1	cctactcatggcttcggcta	tagcggtttgcctggaac
Th	cagggctgctgtcttcctac	gggctgtccagtacgtcaat
ChaT	tcattaatttccgccgtctc	ccggttggtggagtctttta
TPH	cctttgcaagcaagaaggtc	gcatcttggaaggtggtgat

Table 1

Bisulfite genomic sequencing

Genomic DNA for bisulfite sequencing was isolated using the PureGene Genomic DNA isolation kit and bisulfite treatment was performed using Methyl Easy Xceed (human genetic signatures) following the respective manufacturer's protocols. *Oct3/4* promoter region was amplified using ExTaq HS DNA Polymerase. Primers are listed below (Table 2). PCR products were cloned into pGMTEasy (Promega) vector and sequenced with M13 forward primer.

Genes	Forward	Reverse
Oct3/4	caatgggatcctggaggatcctcag	agctctgaggtgtccagggcactat

	attaagtattgggttagtaatgg	taaccctaaacaactactcaacc
	atgggattttggaggatttttag	ctcaaacccaaataccctactt

Table 2

Karyotyping

riPSC were treated with 10μg/mL Colcemid for 3 hours. Cells were trypsinized into a single cell suspension and incubated in 0.075M KCl at 37°C for 15 minutes followed by fixation with ice cold methanol/acetic acid (3:1). Metaphase preparation and chromosome counting were then performed. 100 clones were analyzed for each clone.

Teratoma formation Assay

Animals were purchased from (Japan SLC, Inc). riPSC were typsinized, counted and injected subcutaneously into the neck region of BALB/cSLC-*v*/*v*mice. Tissue masses were harvested after 3-5 weeks, fixed in 4% Paraformaldehyde and sectioned. Sections were stained with hematoxylin and eosin (H&E) according to standard protocols.

Calcium Influx

For Ca^{2+} influx experiments, riPS derived neurons were cultured in poly-L-lysine coated 3.5 cm glass bottom dishes. Neurons were washed once with recording medium (RM): 129 mM NaCl, 4 mM KCl, 1 mM $MgCl_2$, 2 mM $CaCl_2$, 4.2 mM glucose and 10 mM HEPES (pH 7.4), then incubated for 1 h at 37 °C in RM containing 30 nM Pluronic F-127 (Invitrogen) and 1.5 μM fluo-3 acetoxymethyl ester. Culture dishes were then triple washed with Mg^{2+}-free RM and induced fluo-3 Ca^{2+} influx activity visualized at 488 nm with confocal microscope. N-methyl-D-aspartic Acid (NMDA) was added directly onto the medium of the dish undergoing

microscopy to a final concentration of 200μM.

P19 Cell culture and differentiation

Mouse embryonal carcinoma P19 cells were routinely cultured in alpha minimal essential media (α MEM) supplemented with 10% fetal bovine serum (FBS) (Gibco, USA). For differentiation into neural lineage , undifferentiated P19 cells were passaged twice then cultured in low adhesion culture dishes in the presence of 0.5 μ M all trans retinoic acid (ATRA) for 4 days under floating conditions. Cell aggregates formed were dispersed using Accutase, plated onto tissue culture-grade dishes coated with poly-L-lysine for and cultured for 5 days in the absence of ATRA. Cells incubated in a humidified atmosphere containing 5% CO_2 at 37° C at all times and media renewed routinely every 2 days.

RNA isolation and RT-PCR

Total RNA was extracted using Sepazol and genomic DNA removed using DNase 1. 2 μ g RNA was reverse transcribed into cDNA using SuperScript Ⅲ First-Strand Synthesis System for RT-PCR (Invitrogen). cDNA was amplified with THUNDERBIRD SYBR qPCR Mix on a ABI 7500 real time PCR system Samples were run in triplicate and normalized against GAPDH. For semi-quantitative PCR cDNA was amplified using ExTaq. Primers used are shown below.

Genes	Forward	Reverse
Hdac1	ctgtccggtatttgatggct	cacgaactccacacattgg
Hdac2	ggcggcaagaagaaagtgtgc	ggcatcatgtagttcctccagc
Hdac3	tctgaggactacatcgactcc	gtcgccatcatagaaatattg
Hdac8	aacacggctcgatgctgg	ccagctgccacttgatgc

Hes1	cggaatcccctgtctacctct	ttggaatgccgggagctatc
Hes5	gaaaaaccgactgcggaagc	cgaaggctttgctgtgtttca
Musashi1	gaggactcagttggcagacc	tctgtgcctgttggtggttt
CyclinD1	cacaacttctcggcagtcaa	agtgcgtgcagaaggagatt
p21	gcagatccacagcgatatcc	acaccagagtgcaagacagc
NeuroD1	tctgcctcgtgttcctcgt	atgaccaaatcatacagcgagag
Ngn1	ccagcgacactgagtcctg	cgggcataggtgaagtctt
Ngn2	aactccacgtccccatacag	gaggcgcataacgatgcttct
Gapdh(real time)	tgcgacttcaacagcaactc	tgcgacttcaacagcaactc

Table 3

Western blotting

Total protein was extracted from cells using RIPA buffer and lysates centrifuged at 10K×g for 10 minutes at 4° C. Protein samples (10-20 μg) were resolved in 10 or 15% SDS-PAGE gels and transferred to PVDF membranes. Membranes were blocked for 1 h at room temperature and incubated overnight at 4°C with the respective antibodies, followed by application of horseradish peroxidase conjugated secondary antibodies. Proteins were visualized using the chemiluminescent substrate kit and Lumino-Image Analyzer, Las 4000.

REFERENCES

1) Takahashi K, Yamanaka S: Induction of pluripotent stem cells from mouse embryonic and adult fibroblast cultures by defined factors. Cell, 126, 663-676 (2006).

2) Okita K, Ichisaka T, Yamanaka S: Generation of germline-competent induced pluripotent stem cells. Nature, 448, 313-317 (2007).

3) Merkl C, Saalfrank A, Riesen N, Kuhn R, Pertek A, Eser S, Hardt MS, Kind A, Saur D, Wurst W, Iglesias A, Schnieke A: Efficient generation of rat induced pluripotent stem cells using a non-viral inducible vector. PLoS One, 8, e55170 (2013).

4) Liao J, Cui C, Chen S, Ren J, Chen J, Gao Y, Li H, Jia N, Cheng L, Xiao H, Xiao L: Generation of induced pluripotent stem cell lines from adult rat cells. Cell Stem Cell, 4, 11-15 (2009).

5) Li W, Wei W, Zhu S, Zhu J, Shi Y, Lin T, Hao E, Hayek A, Deng H, Ding S: Generation of rat and human induced pluripotent stem cells by combining genetic reprogramming and chemical inhibitors. Cell Stem Cell, 4, 16-19 (2009).

6) Tomioka I, Maeda T, Shimada H, Kawai K, Okada Y, Igarashi H, Oiwa R, Iwasaki T, Aoki M, Kimura T, Shiozawa S, Shinohara H, Suemizu H, Sasaki E, Okano H: Generating induced pluripotent stem cells from common marmoset (Callithrix jacchus) fetal liver cells using defined factors, including Lin28. Genes Cells, 15, 959-969 (2010).

7) Esteban MA, Xu J, Yang J, Peng M, Qin D, Li W, Jiang Z, Chen J, Deng K, Zhong M, Cai J, Lai L, Pei D: Generation of induced pluripotent stem cell lines from Tibetan miniature pig. J Biol Chem, 284, 17634-17640 (2009).

8) Liu J, Balehosur D, Murray B, Kelly JM, Sumer H, Verma PJ: Generation and characterization of reprogrammed sheep induced pluripotent stem cells. Theriogenology, 77, 338-346 e331 (2012).

9) Jacob HJ, Kwitek AE, Gill TJ, 3rd, Smith GJ, Wissler RW, Kunz HW: Rat genetics: attaching physiology and pharmacology to the genome. Nat Rev Genet, 3, 33-42 (2002).

10) Jacob HJ, Lazar J, Dwinell MR, Moreno C, Geurts AM: Gene targeting in the rat: advances and opportunities. Trends Genet, 26, 510-518 (2010).

11) Aitman TJ, Critser JK, Cuppen E, Dominiczak A, Fernandez-Suarez XM, Flint J, Gauguier D, Geurts AM, Gould M, Harris PC, Holmdahl R, Hubner N, Izsvak Z, Jacob HJ: Progress and prospects in rat genetics: a community viewNat Genet, 40, 516-522 (2008).

12) Li P, Tong C, Mehrian-Shai R, Jia L, Wu N, Yan Y, Maxson RE, Schulze EN, Song H, Hsieh CL, Pera MF, Ying QL: Germline competent embryonic stem cells derived from rat blastocysts. Cell, 135, 1299-1310 (2008).

13) Meek S, Buehr M, Sutherland L, Thomson A, Mullins JJ, Smith AJ, Burdon T: Efficient gene targeting by homologous recombination in rat embryonic stem cells. PLoS One, 5, e14225 (2010).

14) Tong C, Huang G, Ashton C, Li P, Ying QL: Generating gene knockout rats by homologous recombination in embryonic stem cells. Nat Protoc, 6, 827-844 (2011).

15) Yamamoto S, Nakata M, Sasada R, Ooshima Y, Yano T, Shinozawa T, Tsukimi Y, Takeyama M, Matsumoto Y, Hashimoto T: Derivation of rat embryonic stem cells and generation of protease-activated receptor-2 knockout rats. Transgenic Res, 21, 743-755 (2012).

16) Li W, Ding S: Generation of novel rat and human pluripotent stem cells by reprogramming and chemical approaches. Methods Mol Biol, 636, 293-300 (2010).

17) Liskovykh M, Chuykin I, Ranjan A, Safina D, Popova E, Tolkunova E, Mosienko V, Minina JM, Zhdanova NS, Mullins JJ, Bader M, Alenina N, Tomilin A: Derivation, characterization, and stable transfection of induced pluripotent stem cells from Fischer344 rats. PLoS One, 6, e27345 (2011).

18) Chang MY, Kim D, Kim CH, Kang HC, Yang E, Moon JI, Ko S, Park J, Park KS, Lee KA, Hwang DY, Chung Y, Lanza R, Kim KS: Direct reprogramming of rat neural precursor cells and fibroblasts into pluripotent stem cells. PLoS One, 5, e9838 (2010).

19) Okita K, Yamanaka S: Induced pluripotent stem cells: opportunities and challenges. *Philos Trans R Soc Lond B Biol Sci,* **366**, 2198-2207 (2011).

20) Jiang MG, Li T, Feng C, Fu R, Yuan Y, Zhou Q, Li X, Wan H, Wang L, Li W, Xiao Y, Zhao XY: Generation of transgenic rats through induced pluripotent stem cells. J Biol Chem, 288, 27150-27158 (2013).

21) Kajiwara M, Aoi T, Okita K, Takahashi R, Inoue H, Takayama N, Endo H, Eto K, Toguchida J, Uemoto S, Yamanaka S: Donor-dependent variations in hepatic differentiation from human-induced pluripotent stem cells. Proc Natl Acad Sci U S A, 109, 12538-12543 (2012).

22) Daley GQ, Lensch MW, Jaenisch R, Meissner A, Plath K, Yamanaka S: Broader implications of defining standards for the pluripotency of iPSCs. Cell Stem Cell, 4, 200-201; author reply 202 (2009).

23) Miura K, Okada Y, Aoi T, Okada A, Takahashi K, Okita K, Nakagawa M, Koyanagi M, Tanabe K, Ohnuki M, Ogawa D, Ikeda E, Okano H, Yamanaka S: Variation in the safety of induced pluripotent stem cell lines. Nat Biotechnol, 27, 743-745 (2009).

24) Koyanagi-Aoi M, Ohnuki M, Takahashi K, Okita K, Noma H, Sawamura Y, Teramoto I, Narita M, Sato Y, Ichisaka T, Amano N, Watanabe A, Morizane A, Yamada Y, Sato T, Takahashi J, Yamanaka S: Differentiation-defective phenotypes revealed by large-scale analyses of human pluripotent stem cells. Proc Natl Acad Sci U S A, 110, 20569-20574 (2013).

25) Bock C, Kiskinis E, Verstappen G, Gu H, Boulting G, Smith ZD, Ziller M, Croft GF, Amoroso MW, Oakley DH, Gnirke A, Eggan K, Meissner A: Reference Maps of human ES and iPS cell variation enable high-throughput characterization of pluripotent cell lines. Cell, 144, 439-452 (2011).

26) Griscelli F, Feraud O, Oudrhiri N, Gobbo E, Casal I, Chomel JC, Bieche I, Duvillard P, Opolon P, Turhan AG, Bennaceur-Griscelli A: Malignant germ cell-like tumors, expressing Ki-1 antigen (CD30), are revealed during in vivo differentiation of partially reprogrammed human-induced pluripotent stem cells. Am J Pathol, 180, 2084-2096 (2012).

27) Riggs JW, Barrilleaux BL, Varlakhanova N, Bush KM, Chan V, Knoepfler PS: Induced pluripotency and oncogenic transformation are related processes. Stem Cells Dev, 22, 37-50 (2013).

28) Andrews PW, Banting G, Damjanov I, Arnaud D, Avner P: Three monoclonal antibodies defining distinct differentiation antigens associated with different high molecular weight polypeptides on the surface of human embryonal carcinoma cells. Hybridoma, 3, 347-361 (1984).

29) Kannagi R, Cochran NA, Ishigami F, Hakomori S, Andrews PW, Knowles BB, Solter D: Stage-specific embryonic antigens (SSEA-3 and -4) are epitopes of a unique

globo-series ganglioside isolated from human teratocarcinoma cells. EMBO J, 2, 2355-2361 (1983).

30) Kannagi R, Levery SB, Ishigami F, Hakomori S, Shevinsky LH, Knowles BB, Solter D: New globoseries glycosphingolipids in human teratocarcinoma reactive with the monoclonal antibody directed to a developmentally regulated antigen, stage-specific embryonic antigen 3. J Biol Chem, 258, 8934-8942 (1983).

31) Schopperle WM, DeWolf WC: The TRA-1-60 and TRA-1-81 human pluripotent stem cell markers are expressed on podocalyxin in embryonal carcinoma. Stem Cells, 25, 723-730 (2007).

32) Kawabe K, Tateyama D, Toyoda H, Kawasaki N, Hashii N, Nakao H, Matsumoto S, Nonaka M, Matsumura H, Hirose Y, Morita A, Katayama M, Sakuma M, Furue MK, Kawasaki T: A novel antibody for human induced pluripotent stem cells and embryonic stem cells recognizes a type of keratan sulfate lacking oversulfated structures. Glycobiology, 23, 322-336 (2013).

33) Ben-David U, Benvenisty N: The tumorigenicity of human embryonic and induced pluripotent stem cells. Nat Rev Cancer, 11, 268-277 (2011).

34) Kaji K, Norrby K, Paca A, Mileikovsky M, Mohseni P, Woltjen K: Virus-free induction of pluripotency and subsequent excision of reprogramming factors. Nature, 458, 771-775 (2009).

35) Nakagawa M, Koyanagi M, Tanabe K, Takahashi K, Ichisaka T, Aoi T, Okita K, Mochiduki Y, Takizawa N, Yamanaka S: Generation of induced pluripotent stem cells without Myc from mouse and human fibroblasts. Nat Biotechnol, 26, 101-106 (2008).

36) Nakagawa M, Takizawa N, Narita M, Ichisaka T, Yamanaka S: Promotion of direct reprogramming by transformation-deficient Myc. Proc Natl Acad Sci U S A, 107, 14152-14157 (2010).

37) Okita K, Yamakawa T, Matsumura Y, Sato Y, Amano N, Watanabe A, Goshima N, Yamanaka S: An efficient nonviral method to generate integration-free human-induced pluripotent stem cells from cord blood and peripheral blood cells. Stem Cells, 31, 458-466 (2013).

38) Sjoberg ER, Varki A: Kinetic and spatial interrelationships between ganglioside glycosyltransferases and O-acetyltransferase(s) in human melanoma cells. J Biol Chem, 268, 10185-10196 (1993).

39) Tateno H, Toyota M, Saito S, Onuma Y, Ito Y, Hiemori K, Fukumura M, Matsushima A, Nakanishi M, Ohnuma K, Akutsu H, Umezawa A, Horimoto K, Hirabayashi J, Asashima M: Glycome diagnosis of human induced pluripotent stem cells using lectin microarray. J Biol Chem, 286, 20345-20353 (2011).

40) Fujitani N, Furukawa J, Araki K, Fujioka T, Takegawa Y, Piao J, Nishioka T, Tamura T, Nikaido T, Ito M, Nakamura Y, Shinohara Y: Total cellular glycomics allows characterizing cells and streamlining the discovery process for cellular biomarkers. Proc Natl Acad Sci U S A, 110, 2105-2110 (2013).

41) Evans MJ, Kaufman MH: Establishment in culture of pluripotential cells from mouse embryos. *Nature,* **292**, 154-156 (1981).

42) Meek S, Wei J, Sutherland L, Nilges B, Buehr M, Tomlinson SR, Thomson AJ, Burdon T: Tuning of beta-catenin activity is required to stabilize self-renewal of rat embryonic stem cells. *Stem Cells,* **31**, 2104-2115 (2013).

43) Buehr M, Meek S, Blair K, Yang J, Ure J, Silva J, McLay R, Hall J, Ying QL, Smith A: Capture of authentic embryonic stem cells from rat blastocysts. *Cell,* **135**, 1287-1298 (2008).

44) Sjoberg ER, Varki A: Kinetic and spatial interrelationships between ganglioside glycosyltransferases and O-acetyltransferase(s) in human melanoma cells. *J Biol Chem,* **268**, 10185-10196 (1993).

45) Dodla MC, Young A, Venable A, Hasneen K, Rao RR, Machacek DW, Stice SL: Differing lectin binding profiles among human embryonic stem cells and derivatives aid in the isolation of neural progenitor cells. *PLoS One,* **6**, e23266 (2011).

46) Li M, Song L, Qin X: Glycan changes: cancer metastasis and anti-cancer vaccines. *J Biosci,* **35**, 665-673 (2010).

47) Cooper O, Hargus G, Deleidi M, Blak A, Osborn T, Marlow E, Lee K, Levy A, Perez-Torres E, Yow A, Isacson O: Differentiation of human ES and Parkinson's disease iPS cells into ventral midbrain dopaminergic neurons requires a high activity form of SHH, FGF8a and specific regionalization by retinoic acid. *Mol Cell Neurosci,* **45**, 258-266 (2010).

48) Warren L, Manos PD, Ahfeldt T, Loh YH, Li H, Lau F, Ebina W, Mandal PK, Smith ZD, Meissner A, Daley GQ, Brack AS, Collins JJ, Cowan C, Schlaeger TM, Rossi DJ: Highly efficient reprogramming to pluripotency and directed differentiation of human cells with synthetic modified mRNA. *Cell Stem Cell,* **7**, 618-630 (2010).

49) Woltjen K, Michael IP, Mohseni P, Desai R, Mileikovsky M, Hamalainen R, Cowling R, Wang W, Liu P, Gertsenstein M, Kaji K, Sung HK, Nagy A: piggyBac transposition reprograms fibroblasts to induced pluripotent stem cells. *Nature,* **458**, 766-770 (2009).

50) Ying QL, Wray J, Nichols J, Batlle-Morera L, Doble B, Woodgett J, Cohen P, Smith A: The ground state of embryonic stem cell self-renewal. *Nature,* **453**, 519-523 (2008).

51) Chen Y, Blair K, Smith A: Robust self-renewal of rat embryonic stem cells requires fine-tuning of glycogen synthase kinase-3 inhibition. *Stem Cell Reports,* **1**, 209-217 (2013).

52) Laurent LC, Ulitsky I, Slavin I, Tran H, Schork A, Morey R, Lynch C, Harness JV, Lee S, Barrero MJ, Ku S, Martynova M, Semechkin R, Galat V, Gottesfeld J, Izpisua Belmonte JC, Murry C, Keirstead HS, Park HS, Schmidt U, Laslett AL, Muller FJ, Nievergelt CM, Shamir R, Loring JF: Dynamic changes in the copy number of pluripotency and cell proliferation genes in human ESCs and iPSCs during reprogramming and time in culture. *Cell Stem Cell,* **8**, 106-118 (2011).

53) Wang YC, Nakagawa M, Garitaonandia I, Slavin I, Altun G, Lacharite RM, Nazor KL, Tran HT, Lynch CL, Leonardo TR, Liu Y, Peterson SE, Laurent LC, Yamanaka S, Loring JF: Specific lectin biomarkers for isolation of human pluripotent stem cells identified through array-based glycomic analysis. *Cell Res,* **21**, 1551-1563 (2011).

54) Gertow K, Przyborski S, Loring JF, Auerbach JM, Epifano O, Otonkoski T, Damjanov I, Ahrlund-Richter L: Isolation of human embryonic stem cell-derived teratomas for the assessment of pluripotency. *Curr Protoc Stem Cell Biol,* **Chapter 1**, Unit1B 4 (2007).

55) Wesselschmidt RL: The teratoma assay: an in vivo assessment of pluripotency. *Methods Mol Biol,* **767**, 231-241 (2011).

56) Knoepfler PS: Deconstructing stem cell tumorigenicity: a roadmap to safe regenerative medicine. *Stem Cells,* **27**, 1050-1056 (2009).

57) Kikuchi T, Morizane A, Doi D, Onoe H, Hayashi T, Kawasaki T, Saiki H, Miyamoto S, Takahashi J: Survival of human induced pluripotent stem cell-derived midbrain

dopaminergic neurons in the brain of a primate model of Parkinson's disease. *J Parkinsons Dis,* **1**, 395-412 (2011).

REFERENCE 2

1) de Ruijter AJ, van Gennip AH, Caron HN, Kemp S, van Kuilenburg AB: Histone deacetylases (HDACs): characterization of the classical HDAC family. Biochem J, 370, 737-749 (2003).

2) Gregoretti IV, Lee YM, Goodson HV: Molecular evolution of the histone deacetylase family: functional implications of phylogenetic analysis. J Mol Biol, 338, 17-31 (2004).

3) Fischer A: Targeting histone-modifications in Alzheimer's disease. What is the evidence that this is a promising therapeutic avenue? Neuropharmacology, 80, 95-102 (2014).

4) Chuang DM, Leng Y, Marinova Z, Kim HJ, Chiu CT: Multiple roles of HDAC inhibition in neurodegenerative conditions. Trends Neurosci, 32, 591-601 (2009).

5) Huangfu D, Osafune K, Maehr R, Guo W, Eijkelenboom A, Chen S, Muhlestein W, Melton DA: Induction of pluripotent stem cells from primary human fibroblasts with only Oct4 and Sox2. Nat Biotechnol, 26, 1269-1275 (2008).

6) Mali P, Chou BK, Yen J, Ye Z, Zou J, Dowey S, Brodsky RA, Ohm JE, Yu W, Baylin SB, Yusa K, Bradley A, Meyers DJ, Mukherjee C, Cole PA, Cheng L: Butyrate greatly enhances derivation of human induced pluripotent stem cells by promoting epigenetic remodeling and the expression of pluripotency-associated genes. Stem Cells, 28, 713-720 (2010).

7) Buggy JJ, Sideris ML, Mak P, Lorimer DD, McIntosh B, Clark JM: Cloning and characterization of a novel human histone deacetylase, HDAC8. Biochem J, 350 Pt 1, 199-205 (2000).

8) Hu E, Dul E, Sung CM, Chen Z, Kirkpatrick R, Zhang GF, Johanson K, Liu R, Lago A, Hofmann G, Macarron R, de los Frailes M, Perez P, Krawiec J, Winkler J, Jaye M: Identification of novel isoform-selective inhibitors within class I histone deacetylases. J Pharmacol Exp Ther, 307, 720-728 (2003).

9) Oehme I, Deubzer HE, Lodrini M, Milde T, Witt O: Targeting of HDAC8 and investigational inhibitors in neuroblastoma. Expert Opin Investig Drugs, 18, 1605-1617 (2009).

10) Deardorff MA, Bando M, Nakato R, Watrin E, Itoh T, Minamino M, Saitoh K, Komata M, Katou Y, Clark D, Cole KE, De Baere E, Decroos C, Di Donato N, Ernst S, Francey LJ, Gyftodimou Y, Hirashima K, Hullings M, Ishikawa Y, Jaulin C, Kaur M, Kiyono T, Lombardi PM, Magnaghi-Jaulin L, Mortier GR, Nozaki N, Petersen MB, Seimiya H, Siu VM, Suzuki Y, Takagaki K, Wilde JJ, Willems PJ, Prigent C, Gillessen-Kaesbach G, Christianson DW, Kaiser FJ, Jackson LG, Hirota T, Krantz ID, Shirahige K: HDAC8 mutations in Cornelia de Lange syndrome affect the cohesin acetylation cycle. Nature, 489, 313-317 (2012).

11) Suzuki T, Ota Y, Ri M, Bando M, Gotoh A, Itoh Y, Tsumoto H, Tatum PR, Mizukami T, Nakagawa H, Iida S, Ueda R, Shirahige K, Miyata N: Rapid discovery of highly potent and selective inhibitors of histone deacetylase 8 using click chemistry to generate candidate libraries. *J Med Chem,* **55**, 9562-9575 (2012).

12) Jones-Villeneuve EM, Rudnicki MA, Harris JF, McBurney MW: Retinoic acid-induced neural differentiation of embryonal carcinoma cells. Mol Cell Biol, 3, 2271-2279 (1983).

13) Shahbazian MD, Grunstein M: Functions of site-specific histone acetylation and deacetylation. Annu Rev Biochem, 76, 75-100 (2007).

14) Haberland M, Montgomery RL, Olson EN: The many roles of histone deacetylases in development and physiology: implications for disease and therapy. Nat Rev Genet, 10, 32-42 (2009).

15) Wang Z, Zang C, Cui K, Schones DE, Barski A, Peng W, Zhao K: Genome-wide mapping of HATs and HDACs reveals distinct functions in active and inactive genes. Cell, 138, 1019-1031 (2009).

16) Yao YL, Yang WM: Beyond histone and deacetylase: an overview of cytoplasmic histone deacetylases and their nonhistone substrates. J Biomed Biotechnol, 2011, 146493 (2011).

17) Saha RN, Pahan K: HATs and HDACs in neurodegeneration: a tale of disconcerted acetylation homeostasis. Cell Death Differ, 13, 539-550 (2006).

18) Sleiman SF, Basso M, Mahishi L, Kozikowski AP, Donohoe ME, Langley B, Ratan RR: Putting the 'HAT' back on survival signalling: the promises and challenges of HDAC inhibition in the treatment of neurological conditions. Expert Opin Investig Drugs, 18, 573-584 (2009).

19) Dietz KC, Casaccia P: HDAC inhibitors and neurodegeneration: at the edge between protection and damage. Pharmacol Res, 62, 11-17 (2010).

20) Bardai FH, D'Mello SR: Selective toxicity by HDAC3 in neurons: regulation by Akt and GSK3beta. J Neurosci, 31, 1746-1751 (2011).

21) Ocker M, Schneider-Stock R: Histone deacetylase inhibitors: signalling towards p21cip1/waf1. Int J Biochem Cell Biol, 39, 1367-1374 (2007).

22) Zhou Q, Dalgard CL, Wynder C, Doughty ML: Histone deacetylase inhibitors SAHA and sodium butyrate block G1-to-S cell cycle progression in neurosphere formation by adult subventricular cells. BMC Neurosci, 12, 50 (2011).

23) Jawerka M, Colak D, Dimou L, Spiller C, Lagger S, Montgomery RL, Olson EN, Wurst W, Gottlicher M, Gotz M: The specific role of histone deacetylase 2 in adult neurogenesis. Neuron Glia Biol, 6, 93-107 (2010).

24) Lyssiotis CA, Walker J, Wu C, Kondo T, Schultz PG, Wu X: Inhibition of histone deacetylase activity induces developmental plasticity in oligodendrocyte precursor cells. Proc Natl Acad Sci U S A, 104, 14982-14987 (2007).

25) Okano H, Kawahara H, Toriya M, Nakao K, Shibata S, Imai T: Function of RNA-binding protein Musashi-1 in stem cells. Exp Cell Res, 306, 349-356 (2005).

26) Ohtsuka T, Sakamoto M, Guillemot F, Kageyama R: Roles of the basic helix-loop-helix genes Hes1 and Hes5 in expansion of neural stem cells of the developing brain. J Biol Chem, 276, 30467-30474 (2001).

27) Kageyama R, Ohtsuka T, Hatakeyama J, Ohsawa R: Roles of bHLH genes in neural stem cell differentiation. Exp Cell Res, 306, 343-348 (2005).

28) Tiberi L, van den Ameele J, Dimidschstein J, Piccirilli J, Gall D, Herpoel A, Bilheu A, Bonnefont J, Iacovino M, Kyba M, Bouschet T, Vanderhaeghen P: BCL6 controls neurogenesis through Sirt1-dependent epigenetic repression of selective Notch targets. Nat Neurosci, 15, 1627-1635 (2012).

29) Hsieh J, Nakashima K, Kuwabara T, Mejia E, Gage FH: Histone deacetylase inhibition-mediated neuronal differentiation of multipotent adult neural progenitor cells. Proc Natl Acad Sci U S A, 101, 16659-16664 (2004).

30) Yu IT, Park JY, Kim SH, Lee JS, Kim YS, Son H: Valproic acid promotes neuronal differentiation by induction of proneural factors in association with H4 acetylation. Neuropharmacology, 56, 473-480 (2009).

ACKNOWLEDGEMENT

My sincere gratitude to my supervisors Professors T. Inazu and Y.Yukio for giving me the opportunity to perform this work. Special thanks to Inazu-sensei for allowing me to be part of your laboratory and introducing me to iPS cell research which has become my passion. Thank you for being patient with me through the research period. Special thanks to Yoneda-sensei for laying the foundation for me as a researcher.

A huge thanks to M. Inden for the technical guidance, material support and friendship. Through your help and advice, I found my footing.

Sincere thanks to Professor T. Kawasaki for providing R-10G and for technical advice and guidance. Thank you to Professors T. Suzuki and N. Miyata for providing HDAC8 inhibitor used. This work would not have been possible without your discoveries.

I am thankful to all members -past and present- of Inazu-ken and in particular Kobayashi M. for your invaluable technical assistance and moral support. Thank you all for many, many, many moments of good cheer.

I am grateful to the Shiga branch Wakken and Nacalai tesque sales representatives, for coming through whenever I needed supplies and answering my ridiculous demands.

Last but not least, I want to thank my family for the support they have given me through this journey. To my beautiful daughter Zawadi, because of you it is all worth it. To mother dearest, I

am because you were.